

OXIDATION CHARACTERISTICS OF SOME
NICKEL ALLOY FILMS

OXIDATION CHARACTERISTICS OF SOME
NICKEL ALLOY FILMS

By

KRISHNA KUMAR GUPTA, M.Sc.

A Thesis

Submitted to the Faculty of Graduate Studies

in Partial Fulfilment of the Requirements

for the Degree

Master of Science

October 1972

MASTER OF SCIENCE
(Physics)

McMASTER UNIVERSITY
Hamilton, Ontario.

TITLE: Oxidation Characteristics of Some Nickel Alloy Films

AUTHOR: Krishna Kumar Gupta, M.Sc. (Lucknow)

SUPERVISOR: Dr. J. Shewchun

NUMBER OF PAGES: vi, 63

SCOPE AND CONTENTS:

The present work is aimed at studying the oxidation of thin films of nickel, nichrome and nickel phosphorous in air and water vapour at temperatures ranging from 100°C to 500°C. The optical constants, i.e., refractive index n and extinction coefficient k for these materials have been determined and their variation with temperature has been studied using ellipsometric technique. It has been shown that nickel oxide (NiO) is the more predominant phase in the oxides formed on these materials. It has also been found that within experimental error, the water vapour does not play a vital role in the oxidation process.

Dedicated to Kamlesh

ACKNOWLEDGEMENTS

I express my sincere thanks for the assistance and supervision given by Dr. J. Shewchun. I also thank Dr. J. P. Marton for his help and guidance throughout the course of this work.

I thank Mrs. H. Kennelly for her patience in typing this thesis.

TABLE OF CONTENTS

	<u>Page</u>	
CHAPTER I	INTRODUCTION	1
CHAPTER II	THEORETICAL	4
	2.1 Plane Waves in Isotropic Media	4
	2.2 Reflection and Transmission of Plane Waves	5
	2.3 Ellipsometry	6
	2.4 Determination of Substrate Optical Constants	12
	2.5 Maxwell Garnett Theory	15
CHAPTER III	EXPERIMENTAL	17
	3.1 Sample Preparation	17
	3.2 Ellipsometer	19
	3.3 Correlation of Experimental Data with Δ and ψ	21
	3.4 Thermal Oxidation of Samples	25
CHAPTER IV	DISCUSSION	28
	4.1 Variation of Substrate Optical Constants	28
	4.2 Effect of Heating in Air and Water Vapour	35
	4.3 Maxwell Garnett Interpretations	38
	4.4 Surface Film Interpretations	42
	4.5 Non-interpretable Data	49
	4.6 Oxidation in Different Oxygen Pressures	50
	4.7 Effect of Water Vapour on Oxides	53
CHAPTER V	CONCLUSIONS	55
APPENDIX I		57
APPENDIX II		59
REFERENCES		61

LIST OF FIGURES

<u>FIGURE NO.</u>		<u>PAGE</u>
1	Symbolic representation of passage of light into an absorbing surface from a non-absorbing medium	7
2	Reflection of light from metallic film on a glass substrate	14
3	Schematic diagram of the ellipsometer	20
4	Variation of Δn with k of oxide film for nickel and nichrome	30
5	Plot of Δ and ψ measured at 70° angle of incidence on Ni, NiP and NiCr samples oxidized at temperatures 300°C and 400°C . Period of oxidation progresses from the right to the left	31
6 (a)	Variation of refractive index of Ni-P with time at temperatures 150°C to 350°C .	33
(b)	Variation of extinction coefficient of Ni-P with time at temperatures 150°C to 350°C	34
7 (a)	Variation of refractive index of Ni, Ni-P and Ni-Cr with time at 400°C	36
(b)	Variation of extinction coefficient of Ni, Ni-P and Ni-Cr with time at 400°C	37
8	Gas desorption and absorption in a NiP sample treated in water-vapour. The data shown is the result of Maxwell Garnett interpretations.	39
9	Absorption and desorption of gases in Ni, Ni-P and Ni-Cr samples heated in air at 200°C	41
10	Oxide film thickness on NiP sample as function of oxidation time at different temperatures in air and water vapour.	43

		<u>Page</u>
11	Oxide film thickness on Ni, Ni-P and Ni-Cr as function of oxidation time in air and water vapour at 400°C	44
12	Film thickness dependence of optical constants of oxide film on Ni-P sample	46
13	(a) Variation of refractive index of oxide films on Ni, Ni-P and Ni-Cr with film thickness. At large thicknesses the value approaches those of NiO.	47
	(b) Variation of extinction coefficient of oxide films on Ni, Ni-P and Ni-Cr with film thickness	48
14	Thickness of oxide film on Ni heated at 300°C and 400°C as a function of oxygen partial pressure	51
15	Thickness of oxide film on Ni, Ni-P and Ni-Cr heated at 400°C for 100 mins. as a function of oxygen partial pressure.	52

CHAPTER I

INTRODUCTION

Optics of metals is, broadly speaking, concerned with the interaction of electromagnetic radiation with conducting media. Optical studies of surfaces have proved to be particularly rewarding as they give valuable information about the optical properties and structure of materials. It has been found that, in most cases, the properties of a thin film are quite different from those of the bulk material⁽¹⁾. This is true of optical, electrical and physical properties. Thin film optics has proved to be a most fascinating field of study.

An optically clean surface is only an idealisation. A very thin oxide film is known to be present on most metals. The optical properties of a metal surface have been shown⁽²⁾ to be modified considerably by the presence of an oxide film or even a monolayer of gas molecules. Surface oxidation directly affects the transport properties and resistivity of metal films, because oxidation contributes scattering centres for the conduction electrons. Oxidation also affects the stability of a resistor. Therefore, an understanding of oxidation mechanism of metal films is required for the fabrication of good quality metal film resistors. The present work is aimed at studying the optical properties and oxidation mechanisms of nickel and two of its alloys,

namely, nickel-phosphorous and nichrome. The knowledge of surface conditions of these materials is important because they are useful for the manufacturing of high precision electrical resistors.

The structure of freshly deposited nickel phosphorous film has been reported⁽³⁾ to be polycrystalline island type. On being heated it undergoes a chemical phase transition, the final products being Ni and Ni_3P ⁽⁴⁾. Marton and Chan⁽⁵⁾ have determined the optical constants (i.e. refractive index n and extinction coefficient k) of Ni-P films annealed in hydrogen to be $n = 2.13$, $k = 2.75$. However, the variation of optical constants with temperature is not known. Effect of heat on Ni-P films has also been studied by Marton and coworkers^(5,6). They found that the oxide grows only above 280°C and that it is a two phase mixture of NiO and P_2O_5 . The optical constants of the oxide were found to depend on thickness of oxide film and were determined to be $n = 1.3$, $k = 0.15$. The effect of water vapour on the oxidation process and the oxide has not been studied so far.

At high temperatures, the oxidation of bulk nickel⁽⁷⁻¹⁰⁾ and nichrome⁽¹¹⁻¹³⁾ has been shown to follow Wagner's parabolic law. Very little is known, however, about the behaviour of thin films of these metals at lower temperatures (below 500°C). Oxidation of nickel in water vapour has been studied by some investigators^(14,15). Though the mechanism of oxidation in

water vapour is not clearly understood, it is known⁽¹⁶⁾ that the rate of oxidation in water vapour is lower than in air by a factor of three. Rahmel⁽¹⁷⁾ studied the oxidation of nickel at 1000°C in oxygen alone and with 43% water vapour. His results indicated that the presence of water vapour does not alter the rate of oxidation. Roberts⁽¹⁸⁾ and Meyerson⁽¹⁹⁾ have determined the optical constants of bulk nickel from reflectance studies to be $n = 1.66$, $k = 3.39$. Roberts also found⁽¹⁸⁾ these constants to be temperature dependent. Optical constants of nichrome have not been reported in the literature so far.

In the present investigation, we have determined optical constants for films of Ni, Ni-Cr and Ni-P (1000-1500 Å) and studied their variation with temperature. In order to gain a better understanding of the oxidation mechanism of Ni-P, we carried out oxidation at temperatures ranging from 100°C to 400°C in different ambients including air, water vapour and gas mixtures in which partial pressure of oxygen was .05 atm and .5 atm respectively. The thickness of the oxide film and its optical constants were calculated in each case. Films of Ni and Ni-Cr (1000-1500 Å) were also subjected to oxidation under similar conditions. We have compared the rates of oxidation and the optical constants of oxides on the three metals. The effect of water vapour on the oxide layer was also studied for Ni, Ni-Cr and Ni-P. The information so obtained throws considerable light on the mechanism and products of oxidation of nickel phosphorous.

CHAPTER II

THEORETICAL

The purpose of this chapter is to present the definitions and theories used in this work. Since most of the theories are well known, no attempt has been made to derive them. Only the end results are given.

2.1 Plane Waves in Isotropic Media

In this section, we will deal with some relations involving the dielectric constant and refractive index of an absorbing medium.

A homogenous, isotropic and absorbing medium can be characterised by a complex index of refraction $\tilde{N} = n - ik$, where n is the ordinary refractive index and k is the extinction coefficient. The equations describing the optical behaviour of a medium are derived from Maxwell's equations by the application of relevant boundary conditions for the medium. We shall generally be concerned with an isotropic, homogenous metal, bounded by plane parallel surfaces. The validity of these assumptions for real metal films, e.g., those deposited by evaporation and chemical deposition, is a question, which we shall not discuss here. We start with a set of plane wave solutions of the Maxwell's equations.

$$\tilde{E} = \tilde{E}_0 \exp i(\tilde{K} \cdot \vec{r} - \omega t) \quad (1)$$

$$\tilde{H} = \tilde{H}_0 \exp i(\tilde{K} \cdot \tilde{r} - \omega t) \quad (2)$$

where \tilde{K} is the propagation vector and is, in general, a complex quantity, i.e., $\tilde{K} = K_1 + iK_2$. For the plane waves defined by (1) and (2), we can show that in a homogenous medium, containing no externally introduced charges or currents, the Maxwell's equations can be written as -

$$\tilde{\mu} \tilde{K} \cdot \tilde{H} = 0 \quad (3)$$

$$\tilde{\epsilon} \tilde{K} \cdot \tilde{E} = 0 \quad (4)$$

$$\tilde{K} \times \tilde{E} = \omega \tilde{\mu} \tilde{H} \quad (5)$$

$$\tilde{K} \times \tilde{H} = -\omega \tilde{\epsilon} \tilde{E} \quad (6)$$

It can be shown that

$$\tilde{K} \cdot \tilde{K} = \epsilon \frac{\omega^2}{c^2}$$

where $\tilde{\epsilon}$ is the complex dielectric constant and is defined by -

$$\begin{aligned} \tilde{\epsilon} &= \epsilon_1 + i \epsilon_2 \\ &= \epsilon_1 + i \frac{\sigma}{\omega \epsilon_0} \end{aligned}$$

The complex refractive index \tilde{N} is then defined as $\tilde{\epsilon} = \tilde{N}^2$, which yields

$$\epsilon_1 = n^2 - k^2 \quad (8)$$

$$\epsilon_2 = 2nk \quad (9)$$

2.2 Reflection and Transmission of Plane Waves

When electromagnetic waves are incident upon a surface, they are reflected and/or transmitted, depending upon the nature of the surface. The reflection and transmission coefficients of

a surface are defined by Fresnel's equations. The four Fresnel's equations are⁽²¹⁾ -

$$r_s = n_1 \cos \phi_2 - \tilde{N} \cos \phi_1 / n_1 \cos \phi_2 + \tilde{N} \cos \phi_1 \quad (10)$$

$$t_s = 2n_1 \cos \phi_2 / n_1 \cos \phi_2 + \tilde{N} \cos \phi_1 \quad (11)$$

$$r_p = n_1 \cos \phi_1 - \tilde{N} \cos \phi_2 / n_1 \cos \phi_1 + \tilde{N} \cos \phi_2 \quad (12)$$

$$t_p = 2n_1 \cos \phi_1 / n_1 \cos \phi_1 + \tilde{N} \cos \phi_2 \quad (13)$$

where all symbols have their usual meanings. (See Fig. 1).

For a thin absorbing film on an absorbing substrate the reflection and transmission coefficients are⁽²²⁾ -

$$\tilde{r} = \tilde{r}_1 + \tilde{r}_2 \exp(2i\delta) / 1 + \tilde{r}_1 \tilde{r}_2 \exp(2i\delta) \quad (14)$$

$$t = \tilde{t}_1 \tilde{t}_2 \exp(i\delta) / 1 + \tilde{r}_1 \tilde{r}_2 \exp(2i\delta) \quad (15)$$

where $\delta = -\frac{2\pi}{\lambda} d \tilde{N} \cos \phi$

r_1 = reflection coefficient at air film surface

r_2 = reflection coefficient at film-substrate interface

t_1 = transmission coefficient at film air surface

t_2 = transmission coefficient at film-substrate interface.

In experiments the measured quantities are $R = n_1 \tilde{r} \tilde{r}^*$ and $T = \tilde{N} \tilde{t} \tilde{t}^*$.

2.3 Ellipsometry

Ellipsometry is considered⁽²³⁾ to be one of the most sensitive techniques for the detection and quantitative measurement of the thickness of contaminant films of oxides, sulphides, etc. on surfaces. In fact it can be used when the film thickness is as small as that of a monoatomic layer or even less, and also when the film is a few thousand angstroms thick. For a historical

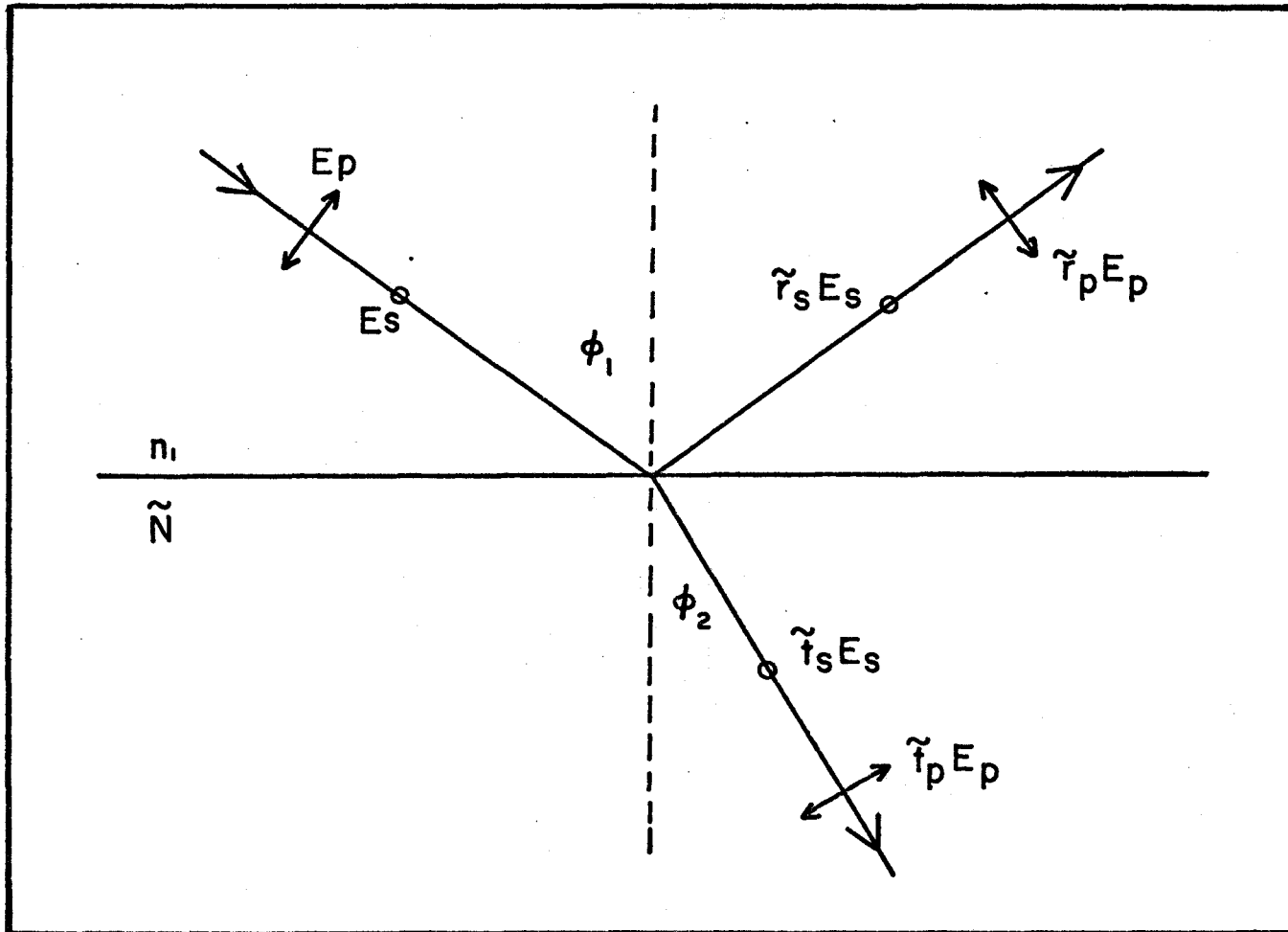


Fig. 1 Symbolic representation of passage of light into an absorbing surface from a non-absorbing medium.

background and other details, interested readers are referred to the literature (24-29).

We have used ellipsometric measurements to determine the optical constants of the metals and their oxides and the thickness of the oxide films. We give a brief discussion of the basic principles involved.

The reflection of light from a metallic surface is found to modify its state of polarisation. Ellipsometry is the measurement of the effect of reflection on the state of polarisation of light. Such measurement can be interpreted to yield the optical constants (i.e. refractive index n and the extinction coefficient k) of the reflecting surface, or when the reflecting material is a film covered substrate, the thickness and optical constants of the film.

We shall consider the reflection of monochromatic, collimated polarised light. The state of polarisation is defined by the phase and amplitude relationship between the two component plane waves, called the p and s components, into which the incident electric vector is resolved. If the p and s components are in phase, the resultant wave is plane polarised. A phase difference other than 0 and 180° corresponds to elliptical polarisation. In general, reflection causes a change in the relative phases of the p and s components and a change in the ratio of their amplitudes.

In practice we consider the case of a beam of plane polarised light striking a film covered surface at an angle of incidence ϕ . If the plane of polarisation in the beam is at 45° to the plane of incidence, the amplitudes of the p and s components are equal. The reflected light is elliptically polarised as the amplitudes and relative phases undergo a change. The effect of reflection is measured by the angle Δ defined as the relative change in phase, and the angle ψ , the arc tangent of the factor by which the amplitude ratio changes. \tilde{r}_p and \tilde{r}_s , being respectively the amplitudes of the p and s components are given by (10) and (12). The relation between \tilde{r}_p , \tilde{r}_s , Δ and ψ is expressed by

$$\frac{\tilde{r}_p}{\tilde{r}_s} = \left| \frac{r_p}{r_s} \right| e^{i\Delta} = \tan \psi \cdot e^{i\Delta} \quad (16)$$

$$\Delta = (\beta_p - \beta_s)_{\text{ref}} - (\beta_p - \beta_s)_{\text{inc}} \quad (17)$$

$$\psi = \arctan \left[\left(\frac{R_p}{R_s} \cdot \frac{E_s}{E_p} \right)_{\text{ref}} / \left(\frac{R_p}{E_p} \cdot \frac{E_s}{R_s} \right)_{\text{inc}} \right] \quad (18)$$

The angles Δ and ψ can be measured with an ellipsometer.

Substitution of (12) into (16) gives

$$\epsilon_1 = n^2 - k^2 = \sin^2 \phi \left[1 + \frac{\tan^2 \phi (\cos^2 2\psi - \sin^2 2\psi \sin^2 \Delta)}{(1 + \sin 2\psi \cos \Delta)^2} \right] \quad (19)$$

$$\epsilon_2 = 2nk = \sin^2 \phi \tan^2 \phi \left[\frac{\sin 4\psi \sin \Delta}{(1 + \sin 2\psi \cos \Delta)^2} \right] \quad (20)$$

The optical constants of a film free surface can be uniquely determined with the help of equations (19) and (20).

When there is a film on the surface, the thickness and optical constants of the film can be calculated from experimentally observed Δ and ψ . Let R_p and R_s be the amplitude reflection coefficients for the film covered surface for the two planes of polarisation. From Eq. (14) we have

$$R_p = \frac{r_{1p} + r_{2p} e^{-2i\delta}}{1 + r_{1p} r_{2p} e^{-2i\delta}} \quad (21)$$

$$R_s = \frac{r_{1s} + r_{2s} e^{-2i\delta}}{1 + r_{1s} r_{2s} e^{-2i\delta}} \quad (22)$$

Dividing (21) by (22) and separating real and imaginary parts, we obtain⁽⁴⁹⁾

$$\tan \Delta = \frac{AB' + A'B}{AA' - BB'} \quad (23)$$

where

$$\left. \begin{aligned} A &= r_{1p} (1 + r_{2p}^2) + r_{2p} (1 + r_{1p}^2) \cos 2\delta \\ A' &= r_{1s} (1 + r_{2s}^2) + r_{2s} (1 + r_{1s}^2) \cos 2\delta \\ B &= -r_{2p} (1 - r_{2s}^2) \sin 2\delta \\ B' &= r_{2s} (1 - r_{1s}^2) \sin 2\delta \end{aligned} \right\} \quad (24)$$

For the azimuth

$$\tan^2 \psi = \frac{(r_{1p}^2 + r_{2p}^2 + 2r_{1p} r_{2p} \cos 2\delta) (1 + r_{1s}^2 r_{2s}^2 + 2r_{1s} r_{2s} \cos 2\delta)}{(1 + r_{1p}^2 r_{2p}^2 + 2r_{1p} r_{2p} \cos 2\delta) (r_{1s}^2 + r_{2s}^2 + 2r_{1s} r_{2s} \cos 2\delta)} \quad (25)$$

To obtain refractive index of the film \tilde{N} and thickness d , equations (23) and (25) have to be solved. These equations cannot

be solved to give explicit expressions for \tilde{N} and d . Since all r 's involve \tilde{N} and $\cos 2\delta$ terms involve $\tilde{N}d$. The solution becomes even more difficult if both the film and the substrate are absorbing as in that case where the refractive indices for both are complex quantities. These transcendental equations can be solved with the help of a digital computer only. If the optical constants of the film and the substrate are known, then the film thickness can be calculated by solving equation (25) which is a quadratic in $\cos 2\delta$ with the observed ψ to evaluate δ . The thickness ' d ' can thus be determined.

If, however, the optical constants of the film are not known, it is not possible to get a direct and unique solution for both \tilde{N} and d . The procedure now adopted is to choose a likely value of \tilde{N} and use Eq. (25) to calculate d . Equations (23) and (24) then enable Δ to be calculated for the chosen \tilde{N} . This procedure is repeated for a number of values of \tilde{N} . The value of \tilde{N} for which the calculated value of Δ is closest to the observed Δ , gives the optical constants of the film. The film thickness corresponding to this value of \tilde{N} can now be calculated from Eqn. (25).

We used McCrackin and Colson's⁽³⁰⁾ computer program for evaluating the film thickness and its optical constants from the observed ellipsometric parameters Δ and ψ . This

program has been designed to go through the iterative process outlined above. Similar techniques have been used by earlier workers⁽⁵⁾ to calculate the film parameters.

2.4 Determination of Substrate Optical Constants

The problem of determination of optical constants of a pure metal surface has attracted much attention. A bare metal surface exposed to air is likely to grow an oxide film and/or adsorb gas molecules on the surface, thereby changing the optical properties of the surface. We will now consider methods for determination of optical constants of a metal surface, called the substrate, covered by an absorbing oxide film.

Some workers have tried to determine the substrate optical constants by correcting for the effects of surface films^(2,26,31-33). Reflectance studies at various angles of incidence have also been employed⁽³⁴⁾. Recently multiple angle of incidence method has been used with considerable success^(35,36). However these methods can be used successfully only in cases where the film is non absorbing or only slightly absorbing. In the present work, we used multiple angle of incidence method as modified by Shewchun and Rowe⁽³⁵⁾. However, it was found necessary to

modify their computer program to obtain convergence in the presence of an absorbing oxide film. The other method used was second surface reflection, in which the optical constants of the metal were determined by studying the reflection at the glass-metal interface. The metal surface in contact with glass is not exposed to the atmosphere and can be relied upon to yield optical constants of the unoxidised metal. We used these two methods as they were considered more accurate. The study also provides a comparison between the optical constants obtained by the two methods.

In the second surface reflection method⁽⁴⁸⁾, we consider a beam of plane polarised light, with the plane of polarisation at 45° to the plane of incidence, incident at the glass surface at an angle of incidence ϕ_0 . We study the first reflected beam from metal surface marked II in Fig. (2). In this beam, the amplitudes of p and s components are given by⁽²²⁾ -

$$R_p = t_p t'_p r_{2p} \quad (26)$$

$$R_s = t_s t'_s r_{2s} \quad (27)$$

To get the free surface angles $\bar{\phi}, \bar{\Delta}$ and $\bar{\psi}$ from the observed ϕ_0, Δ_0 and ψ_0 , we used the following relations (see Appendix 1)-

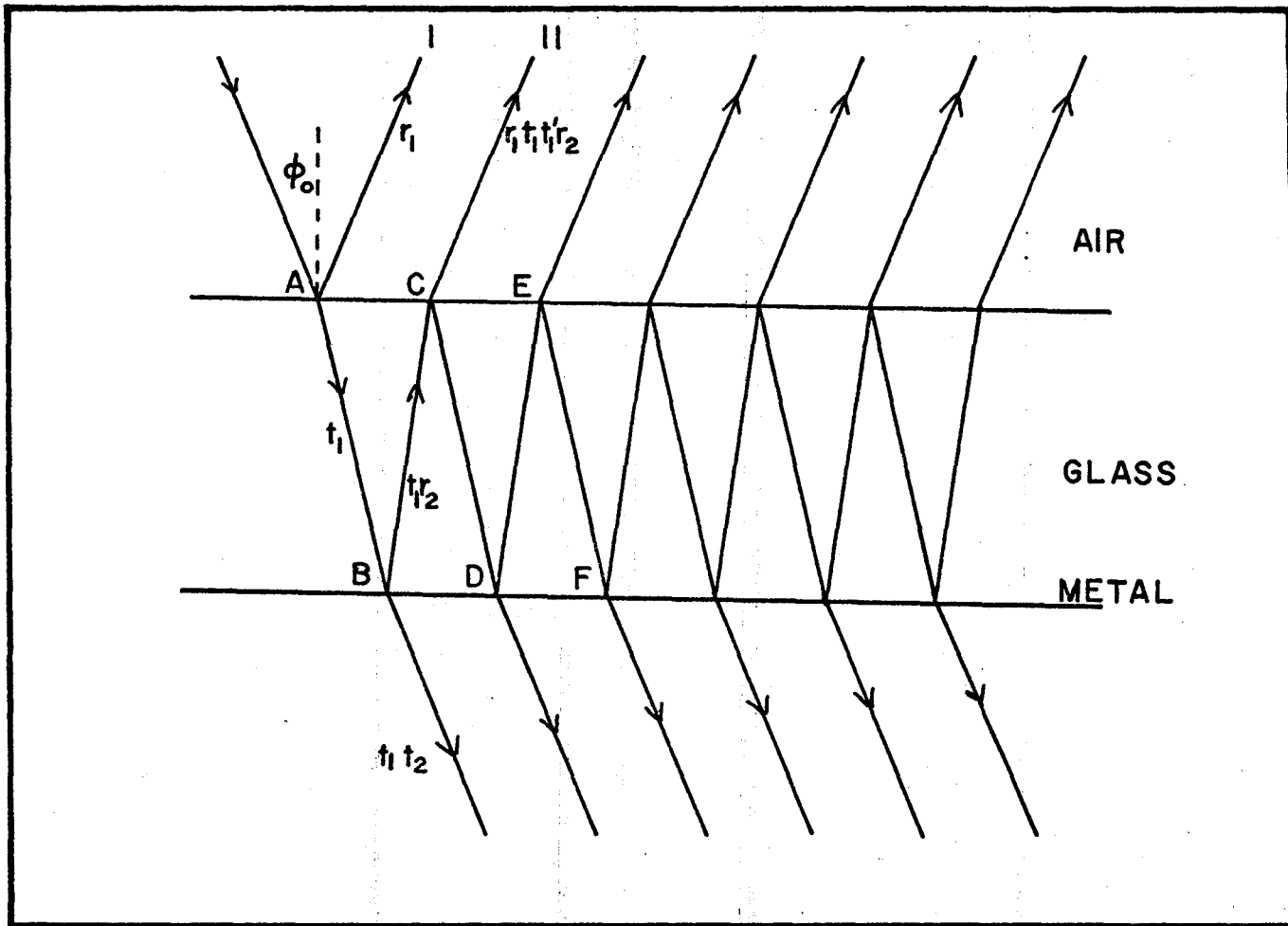


Fig. 2 Reflection of light from metallic film on a glass substrate .

$$\bar{\phi} = \phi_1 = \sin^{-1} \left[\frac{\sin \phi_o}{n_1} \right] \quad (28)$$

$$\bar{\Delta} = \Delta_o \quad (29)$$

$$\bar{\psi} = \tan^{-1} \left[\tan \psi_o \frac{t_s t'_s}{t_p t'_p} \right] \quad (30)$$

where n_1 is the refractive index of glass.

Having determined the free surface angles, the optical constants of the oxide free metal surface were calculated using equations (19) and (20).

2.5 Maxwell Garnett Theory

As stated earlier, the absorption or desorption of gases on the surface of a thin metallic film, where the ratio of its volume to its exposed surface is extremely small, may be critical to its optical properties. The change in the optical properties of a surface may be interpreted with the help of the Maxwell Garnett theory in terms of a gas exchange at the surface.

The optical properties of a system consisting of a large number of spherical metal particles, of diameter small compared with wavelength of light used and embedded in a dielectric medium, were investigated by Maxwell Garnett⁽³⁷⁾. According to his theory, a thin film may be represented by a random distribution of spherical metal crystallites of diameter small compared with the film thickness. The density of the film is characterised by the aggregation parameter 'q' which gives the fractional volume occupied by the metal. When an electromagnetic wave traverses such a system, the spherical crystallites will be polarised by the electric field of the wave and will thus

produce an additional field E_s . This field may be calculated in precisely the way in which the polarisation field in a dielectric is determined (see Appendix II). The thin film may be represented by a volume fraction q of metallic spheres of index \tilde{N} in a medium of refractive index very close to unity. The effective index \tilde{N}_e of the system is then given by

$$\frac{\tilde{N}_e^2 - 1}{\tilde{N}_e^2 + 2} = 'q' \frac{\tilde{N}^2 - 1}{\tilde{N}^2 + 2} \quad (31)$$

The effective index \tilde{N}_e may be determined with an ellipsometer. The observed ψ and Δ at the free surface of the sample were used to calculate the optical constants of the surface. It is assumed that the optical constants so obtained represent \tilde{N}_e . The validity of this assumption is, however, questionable. It is also assumed that the constituent metal crystallites have the same optical constant \tilde{N} as that of the bulk metal. The optical constants (i.e., the complex refractive index $\tilde{N} = n - ik$) of the metal were in each case determined by back reflection method described earlier. Thus knowing \tilde{N} and \tilde{N}_e for a sample, we can calculate the aggregation parameter 'q'. An increase in 'q' is taken to represent desorption of gases at the surface while a decrease in 'q' indicates absorption.

CHAPTER III
EXPERIMENTAL

In this chapter we will present experimental details relating to preparation of samples, heating them in different ambients and their study with an ellipsometer.

3.1 Sample Preparation

Nickel and nichrome films were made by thermal evaporation of these metals in vacuum on glass substrates. Pyrex glass substrates, one inch square and a quarter inch thick, were used throughout the experiment. The substrates were cleaned with hot chromic acid and distilled water. A cold rolled sheet of polycrystalline nickel, prepared direct from electrolytic cathode was obtained through the courtesy of the Department of Metallurgy and Materials Science, McMaster University, Hamilton. It was first chemically polished by heating for about two mins. at 80°C in a solution whose composition is given below.

TABLE 1

Composition of solution for chemical polishing of nickel

Nitric acid (Conc.)	30 ml.
Sulphuric acid (Conc.)	10 ml.
Ortho phosphoric acid	10 ml.
Acetic acid (ice cooled)	50 ml.

The specimen was washed with distilled water and then electropolished in a 60% H_2SO_4 solution for about 30 sec. at 1 amp./cm.². A platinum strip of the same area as the specimen was used as the cathode. The specimen was then washed with distilled water and dried in air.

A NRC 3116 vacuum coater, with an alumina coated tungsten boat as source, was used for evaporation. Deposition was carried out at room temperature at the rate of about 200 Å per min. Thickness of deposit was continuously monitored by a SLOAN-OMNI II deposit control master. A shutter was used to prevent condensation of any gases at the substrates, evolved from the source during initial period of heating. We found that use of the shutter and prolonged degassing of substrate was required in order to make a good deposit, otherwise the film was found to be less aggregated at the glass metal interface than at the free surface. It was not possible to deposit nickel films thicker than ≈ 1500 Å. As the films grew thicker, they started to crack and peel off from the substrate. This could be due to poor adhesive characteristics of nickel to glass or development of strains in the film.

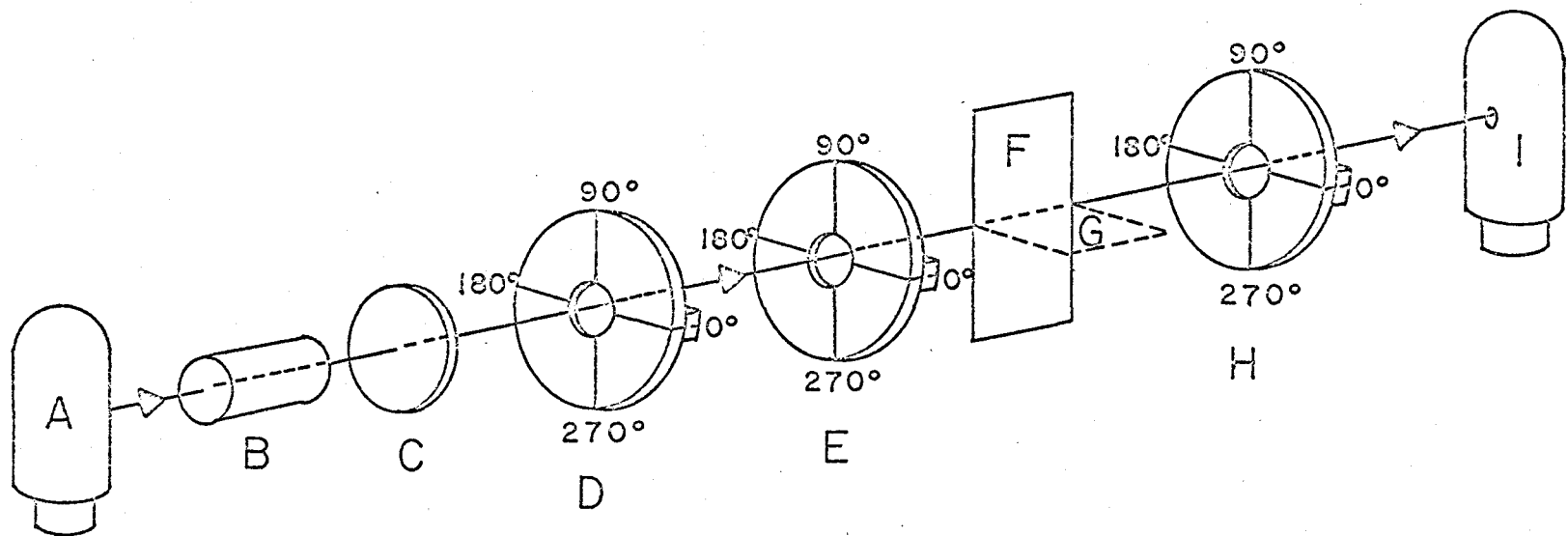
Nichrome films were made by thermal evaporation of nichrome (Ni 80%, Cr 20%) obtained through the courtesy of Garret Manufacturing Co., Toronto. The cleaning and deposition procedures were the same as that for nickel. For nichrome also it was found difficult to deposit films thicker than ≈ 1200 Å.

Reasons for the cracking and peeling of films are not completely understood.

Nickel-phosphorous films were made by electroless deposition of the metal on pyrex glass substrates. For cleaning and activation of substrates and deposition of Ni-P, we followed accepted procedures^(38,39). Thickness of Ni-P deposit can be controlled by the deposition time. We allowed the deposition to continue for two hours for all samples. The thickness of the deposit as measured by the Angstrommeter was in the range of 1000 - 1200 Å. The Ni-P deposit was removed from one side of the glass substrate by rubbing the surface with aqua-regia. This was necessary in order to enable ellipsometric measurements to be made at the glass metal interface by second surface reflection.

3.2 Ellipsometer

A schematic diagram of the ellipsometer is given in Fig. (3). Light from a mercury vapour lamp first passes through a filter and collimating lens system, producing a parallel beam of monochromatic light about 6 mm. in diameter (wavelength 5461 Å). It then passes through a polarising nicol prism followed by a variable diaphragm which can vary the diameter of the beam from 1 mm. to 6 mm. When the plane of polarisation is set at an azimuth of 45° to the plane of incidence, one of its components propagates in the plane of incidence and the other perpendicular to it, each with equal intensity. When the



- A. Mercury lamp
- B. Filter (5461Å)
- C. Collimator
- D. Polarizer
- E. Compensator

- F. Sample
- G. Plane of incidence
- H. Analyser
- I. Photo-multiplier

Fig. 3 Schematic diagram of the Ellipsometer.

compensator is mounted before the sample, the plane polarised light, upon passing through the compensator, is elliptically polarised before striking the surface of the sample. Upon reflection the light is linearly polarised and is analysed with an analysing nicol prism followed by a photomultiplier tube and associated metering electronics used as the detector.

Measurements were made by first setting the compensator at 45° . The polariser and analyser were then adjusted to obtain null point in the detector. Usually the null point is too broad to permit accurate measurement. Therefore an equal deflection method, successfully employed by other workers^(5,35), was used. To determine Δ and ψ from the ellipsometric observations of polariser angle P and analyser angle A, a method similar to McCrackin Zone scheme⁽²⁹⁾ was used.

3.3 Correlation of Experimental Data with Δ and ψ

In general, for a given surface, there is a multiplicity of polariser, analyser and compensator settings that produce extinction by the analyser of the reflected light from the surface. The various readings fall into four separate sets called the four zones. When the fast axis of the compensator is fixed at $\frac{\pi}{4}$, the zones are numbered 2 and 4, while with the fast axis at $-\frac{\pi}{4}$ the two zones are numbered 1 and 3. In each zone there is one P and A reading which would achieve extinction. However, both polariser and analyser can be rotated by 180° without affecting the results, therefore, there are 16 P and A settings

in the four zones. Also, the compensator can be rotated by π without changing the azimuth. Hence, there are 32 possible sets of P and A settings for one angle of incidence. A zone scheme has been given by Winterbottom⁽²⁷⁾ for the utilisation of the instrument readings. The results are listed below:-

Zone 1 - The fast axis of the compensator is at $-\frac{\pi}{4}$. The polariser plane of transmission makes an angle of $+p$ with the plane of incidence. The analyser plane of transmission makes an angle of $+a_p$ with the plane of incidence.

Zone 2 - The fast axis of the compensator is at $\frac{\pi}{4}$. The polariser plane of transmission makes an angle of $-p$ with the reflecting surface (or $\frac{\pi}{2} - p$ with the plane of incidence). The analyser plane of transmission makes an angle of $+a_s$ with the plane of incidence.

Zone 3 - The fast axis of the compensator is fixed at $-\frac{\pi}{4}$. The polariser plane of transmission makes an angle of $+p$ with the surface (or an angle of $\frac{\pi}{2} + p$ with the plane of incidence). The analyser plane of transmission makes an angle of $-a_s$ with the plane of incidence.

Zone 4 - The fast axis of the compensator is at $\frac{\pi}{4}$. The polariser plane of transmission makes an angle of $-p$ with the plane of incidence. The analyser plane of transmission makes an angle of $-a_p$ with the plane of incidence.

With these relationships, the relation of P and A to a_p , a_s and p may be found from Table 2.

TABLE 2

Relation of P and A readings with a_p , a_s and p

Zone	Compensator	P	A
1	$-\pi/4$	p	a_p
		$p+\pi$	a_p
		p	$a_p+\pi$
		$p+\pi$	$a_p+\pi$
3	$-\pi/4$	$p+\pi/2$	$\pi-a_s$
		$p+3\pi/2$	$\pi-a_s$
		$p+\pi/2$	$2\pi-a_s$
		$p+3\pi/2$	$2\pi-a_s$
2	$+\pi/4$	$\pi/2-p$	a_s
		$3\pi/2-p$	a_s
		$\pi/2-p$	$a_s+\pi$
		$3\pi/2-p$	$a_s+\pi$
4	$+\pi/4$	$\pi-p$	$\pi-a_p$
		$2\pi-p$	$\pi-a_p$
		$\pi-p$	$2\pi-a_p$
		$2\pi-p$	$2\pi-a_p$

For the case of an exact quarter wave plane, i.e., one whose fast and slow axis are exactly perpendicular to each other, the parameters Δ and ψ are related to the polariser angle P and the analyser angle A by the relations -

$$\psi = a_p = a_s \quad (27)$$

$$\Delta = \frac{\pi}{2} + 2p$$

Archer⁽²⁶⁾ has shown that for a non-exact quarter wave plate, the ellipticity is given by

$$\tan^2 \psi = \tan a_p \cdot \tan a_s \quad (29)$$

and the phase change is given by

$$\tan \Delta = -\sin \delta \cdot \cot 2P \quad (30)$$

where δ is the retardation of the quarter wave plate.

In actual practice, the values of p , a_p and a_s in the various zones are not the same. The reason for disagreement of the p readings in the four zones is not clearly understood. The variation of a_p and a_s in the different zones arises because of inaccuracy in the quarter wave plate. In actual practice, only one set of P and A readings was taken in each zone, because in general the difference of P and A readings within a zone was of the order of ± 0.01 degree, which does not significantly affect the results. Δ and ψ obtained from the four zones were averaged. Measurements were carried out at two angles of incidence lying between 65° to 75° .

3.4 Thermal Oxidation of Samples

In the present study we have used the isothermal method for thermal oxidation of samples. This consisted of making a number of runs at various temperatures under different conditions. The samples to be heated at different temperatures are required to be initially identical, a condition which is difficult to achieve in the case of thin films. The fair amount of spread in the optical constants of films of the same material indicates that samples prepared under similar conditions are not identical.

Samples of nickel, nichrome and nickel phosphorous were subjected to heat treatment at temperatures ranging from 100°C to 500°C. This was done in different ambients including air, saturated water vapour and two oxygen-nitrogen mixtures. The experimental arrangement consisted of a quartz tube, 3" in diameter, placed in a low temperature three-zone furnace. A quartz boat was used to introduce the sample. The temperature gradient along the length of the boat was determined to be less than 1%. It was found that a pre-heating time of about one hour was required by the furnace. After heating the sample was withdrawn from the tube and allowed to cool in the air at room temperature

For heating the samples in water vapour, steam, obtained by boiling deionised water, was passed through the tube at a constant rate, enough to keep the volume of the tube saturated with steam. The other end of the tube was closed with a ground

glass cap with an exit. This allowed any water or steam to escape but prevented the re-entry of air. In order to ensure that all the air was removed, steam was allowed to flow in the system for about 30 mins. before introducing the sample.

Besides heating in air and water vapour, the samples were heated in two oxygen-nitrogen mixtures. In the first case, pure oxygen at 1 lb. pressure was mixed with nitrogen at 20 lb. pressure. The partial pressure of oxygen in this mixture is about .05 atm. The degree of accuracy attainable in making this mixture is only approximate as the pressure gauges used read a minimum of 2 lb./div. The other mixture was obtained by mixing both oxygen and nitrogen at 10 lb. pressure, giving a .5 atm. partial pressure of oxygen. The quartz tube was flushed with the gas mixture for 15 mins. to remove air. The sample was then heated with the gas mixture flowing continuously through the tube.

Heating of nichrome samples in air presented some difficulty. On heating nichrome films in air, we found that dark dots and lines appeared on the surface and their density increased with time and temperature. This might be due to cracking of the film as a result of structural defects and/or associated strains. No such problem was encountered in the heating of nickel or Ni-P or nichrome in water vapour. When nickel films were heated at 400°C for periods exceeding 200 mins. they started

losing their opacity and were no longer considered fit for ellipsometric measurements. This could be overcome by using thicker films. The practical difficulty in depositing thicker films has been discussed earlier.

CHAPTER IV

DISCUSSION

When films of nickel, nichrome and nickel phosphorous are heated in air or water vapour, one or more of the following changes are found to occur -

- a. Change in the optical constants of the metal.
- b. Absorption or desorption of gases at the surface.
- c. Growth of a surface oxide film which may or may not be accompanied by a change of colour of the surface.

It has been pointed out earlier that samples prepared under similar conditions are not identical. The optical constants reported here are averages of over ten samples. We found that when two samples were subjected to similar treatment, the thickness of oxide layer varied up to $\pm 10\%$. For oxidation studies we studied three samples under similar conditions and the results reported are averages of three samples in each case.

4.1 Variation of Substrate Optical Constants

Two methods, namely, multiple angle of incidence and second surface reflection, were used to determine substrate optical constants and study their variation with temperature. The results obtained from the two methods agreed closely (within 10%) only when the oxide was non absorbing or only very

slightly absorbing ($k \approx 0.05$). When the oxide was more absorbing, the results varied by 20 - 25% or more. In such cases, the results obtained from second surface measurements were considered more reliable. The variation of Δn , where

$$\Delta n = n_{\text{mult.angle}} - n_{\text{back ref.}}$$

with extinction coefficient 'k' of the oxide for nickel and nichrome is shown in figure (4).

We studied films of nickel, nichrome and nickel phosphorous 1000 to 1200 Å thick. Optical constants of freshly deposited nickel films were determined to be $n = 1.9 \pm 0.1$ and $k = 3.5 \pm 0.1$. When they were heated in air and water vapour, both n and k showed a decrease saturating at $n \approx 1.7$ and $k \approx 3.4$. Meyerson⁽¹⁹⁾ has reported the optical constants of bulk nickel to be $n = 1.66$, $k = 3.39$. It appears that the optical constants of a 1000 Å film are not much different from the bulk metal at the wavelength of light used. Sennett and Scott found⁽³⁹⁾ that transmission coefficients for nickel films thicker than 100 Å are nearly the same.

Optical constants of nichrome (Cr 20%, Ni 80%) have not been reported so far in the literature. An estimate made from the optical constants of nickel and chromium yielded $n = 2.12$, $k = 3.48$. Using ellipsometric technique, we determined the optical constants of nichrome films (1000-1500 Å) to be $n = 2.5 \pm 0.1$, $k = 3.4 \pm 0.1$. When these films were heated in air and water vapour, n decreased and k increased, both

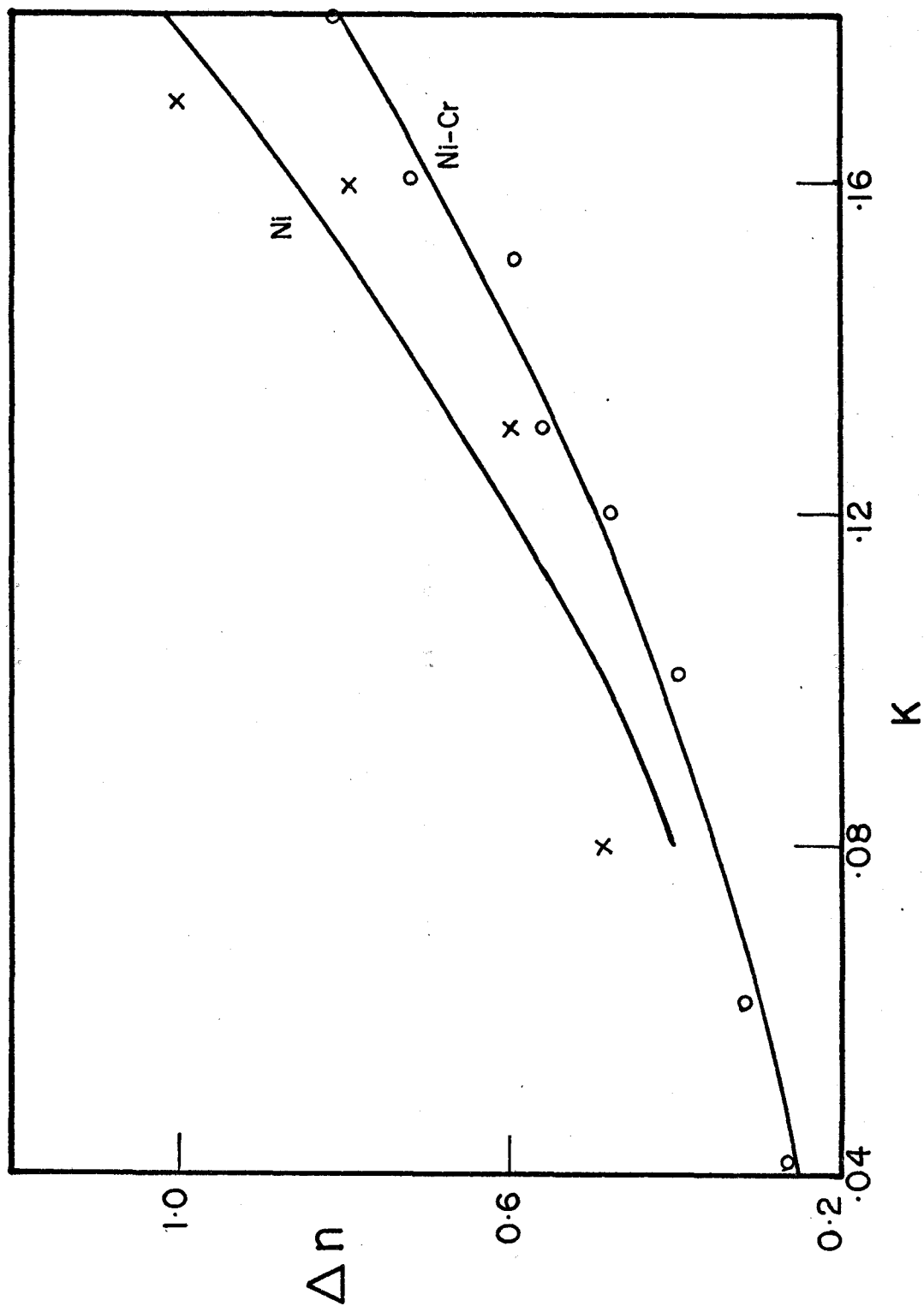


Fig. 4 Variation of Δn with k of oxide film for nickel and nichrome.

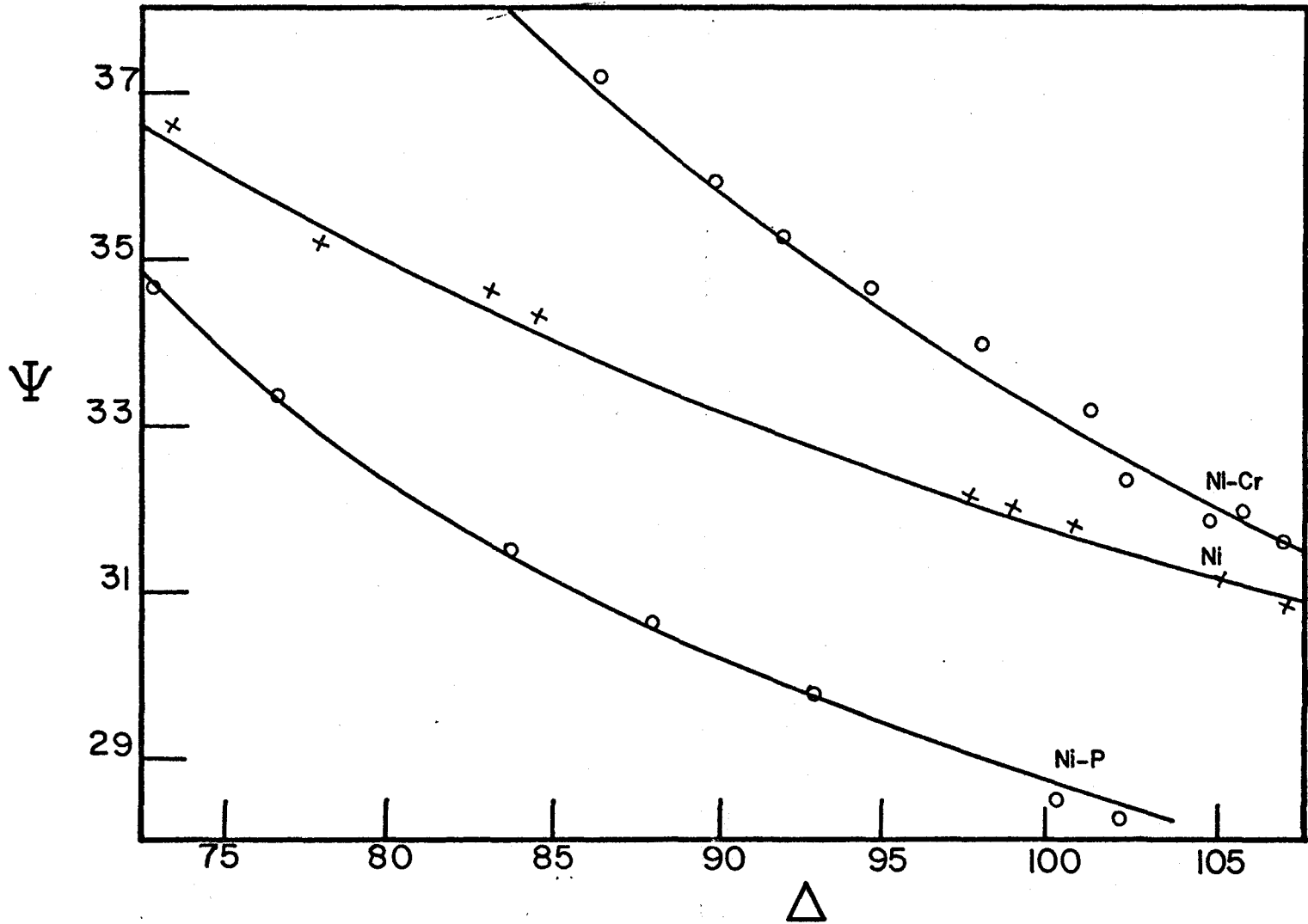


Fig. 5 Plot of Δ and ψ measured at 70° angle of incidence on Ni, NiP and NiCr samples oxidized at temperatures 300°C and 400°C . Period of oxidation progresses from the right to the left.

saturating at longer times. The saturation values were found to be $n = 2.25$, $k = 3.48$. The experimentally determined values ($n = 2.25$, $k = 3.48$) compare favourably with the theoretically estimated ones and those found by Shewchun⁽⁴⁰⁾ ($n = 2.33$, $k = 3.48$).

For freshly deposited Ni-P films, we determined the optical constants to be $n = 2.6 \pm 0.1$, $k = 2.6 \pm 0.1$. When the films were heated in air, the optical constants showed a change similar to that in nichrome. The saturation values of the optical constants in air were $n = 2.15$, $k = 2.78$. When the films were heated in water vapour, the change in optical constants was similar. However, the saturation values of the optical constants were found to be $n = 2.35$, $k = 2.92$. The saturation values of optical constants ($n = 2.15$, $k = 2.78$) compare favourably with those reported by Marton and Chan⁽⁵⁾ ($n = 2.13$, $k = 2.75$) for Ni-P films annealed in hydrogen.

Ni-P films are known to undergo compositional and crystalline changes on being heated. Pai and Marton have found⁽⁴⁾ that initially the Ni-P film is a fine grain polycrystalline material. Upon heating the film is transformed into a two phase mixture of Ni and Ni₃P. These changes may also account for the observed variation in optical constants. Roberts⁽¹⁸⁾ and Ward⁽⁴¹⁾ also have reported the temperature dependence of optical properties of nickel. Adams and Rao⁽⁴²⁾ have suggested that the change in optical properties of thin films on heating may be due to annealing of defects. It is logical to assume

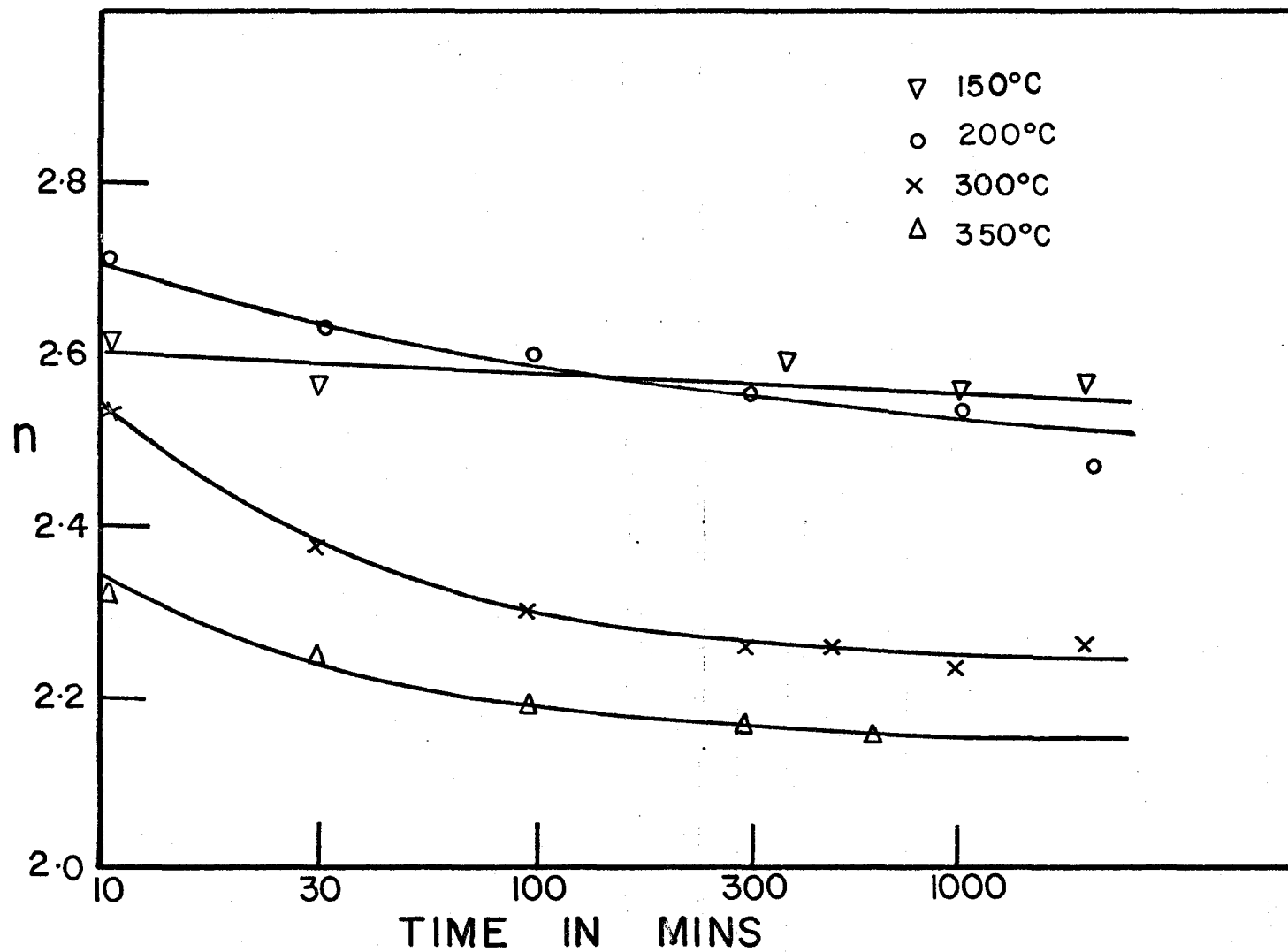


Fig. 6(a) Variation of refractive index of Ni-P with time at temperatures 150°C to 350°C.

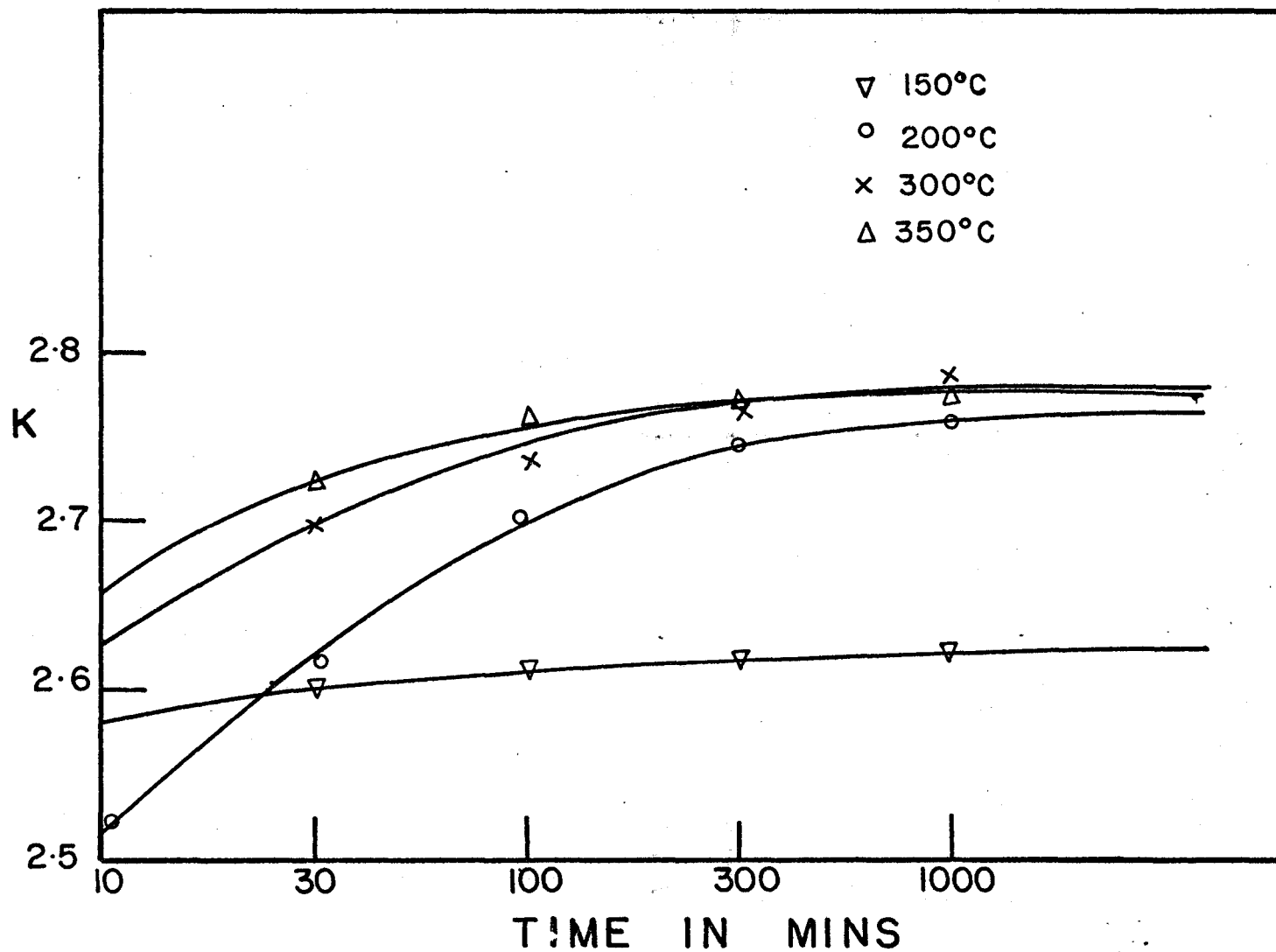


Fig. 6(b) Variation of extinction coefficient of Ni-P with time at temperatures 150°C to 350°C

that similar phenomenon would be responsible for a change in optical constants of nichrome on heating.

A typical set of data showing variation of n and k for Ni-P at various temperatures is shown in figs. 6(a) and 6 (b) Figs. 7(a) and 7(b) show variation of n and k for Ni, Ni-Cr and Ni-P at 400°C.

4.2 Effect of Heating in Air and Water Vapour

Films of nickel, nichrome and nickel phosphorous 1000-1500 Å thick were subjected to heat treatment in air and water vapour at temperatures ranging from 100°C to 400°C. The ellipsometric data on heated samples can generally be divided into three categories. For lower temperatures of heat treatment, i.e., 100°C to 250°C, we found that observed Δ and ψ were not interpretable in terms of a surface oxide film. However these Δ and ψ readings could be interpreted with the help of Maxwell Garnett theory as a change in optical properties of the film surface caused by absorption or desorption of gases.

For temperatures of heat treatment above 300°C, we could interpret the observed Δ and ψ in terms of a surface oxide film. We found, however, that the observed data on Ni-P samples heated in air at 400°C for periods longer than 100 mins. could not be interpreted by any of the available methods. A similar problem was encountered in the analysis of data for nickel samples heated at 400°C for longer periods of time.

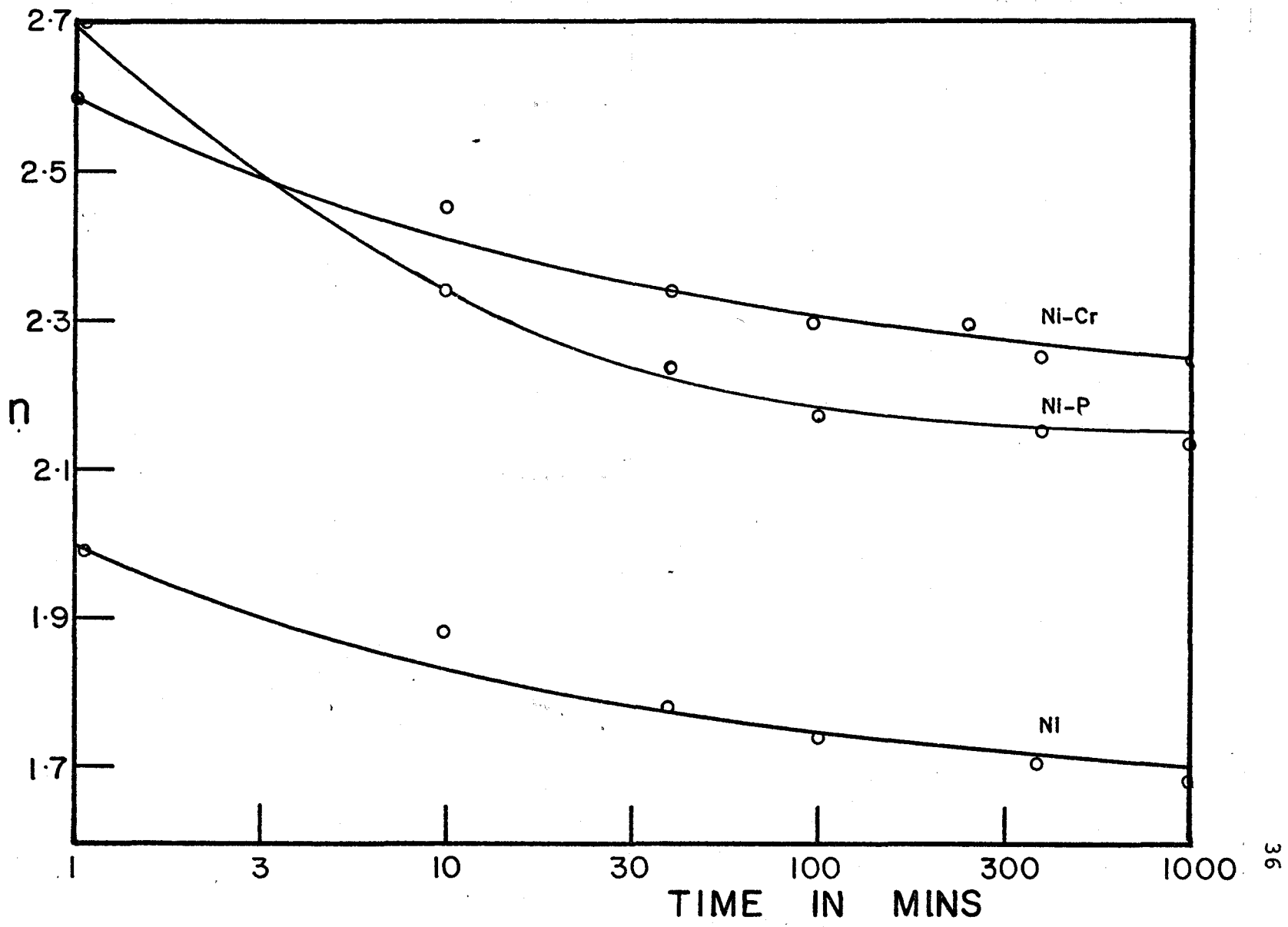


Fig. 7(a) Variation of refractive index of Ni, Ni-P and Ni-Cr with time at 400°C.

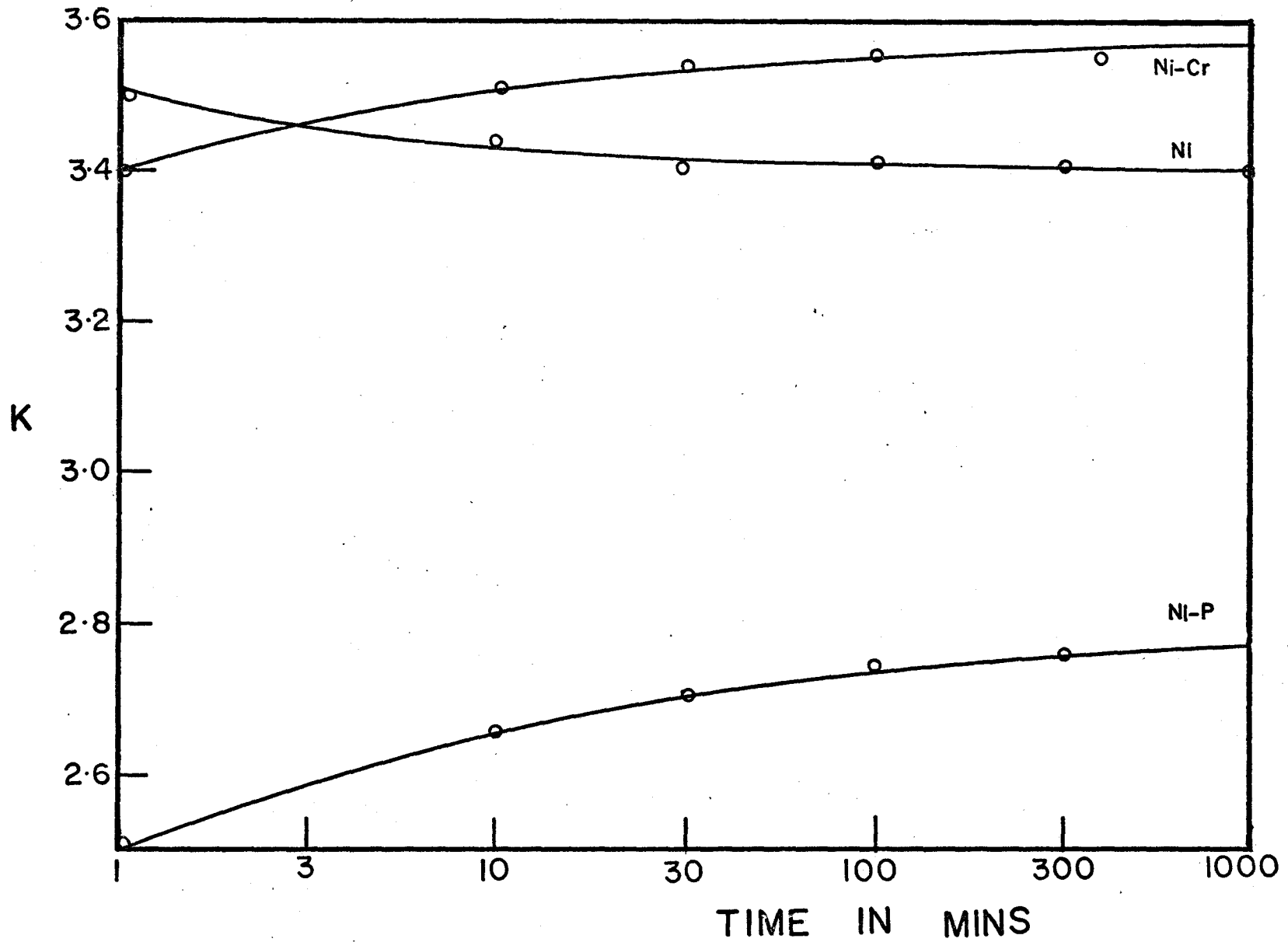


Fig. 7b Variation of extinction coefficient of Ni, Ni-P and Ni-Cr with time at 400°C.

4.3 Maxwell Garnett Interpretations

Marton and Chan⁽⁵⁾ have used Maxwell Garnett theory to analyse the changes in the optical constants of a nickel-phosphorous surface in terms of absorption and desorption of gases. Lederich and Bellina⁽⁴³⁾ have also used a similar method to study niobium metal. We have used the Maxwell Garnett theory to analyse the experimental data on samples of nickel, nichrome and nickel phosphorous heated at temperatures below 300°C. Values of aggregation parameter 'q' were calculated from \tilde{N} and \tilde{N}_e for a sample after each period of heating. It is seen from Eqn. (31) that an increasing 'q' value represents desorption of impurities (e.g. N₂ and H₂) and a decrease in 'q' value represents absorption of impurities (e.g. oxygen). The fluctuation of the 'q' curve may be explained in terms of a desorption-absorption process at the surface. In Fig. (8), we have presented a typical set of data for Ni-P sample heated in water vapour at various temperatures. For nickel films heated in air at 100°C and 200°C, there is indication of desorption at the surface in the initial stages while absorption takes place after about 100 mins. The desorption could be due to nitrogen from the atmosphere getting trapped in the film at the time of deposition. This gas could escape from the film on heating. Oxygen is absorbed continuously later on but no oxide film was detected on the surface for periods of heating as long as 300 mins. When Ni films were heated in water vapour,

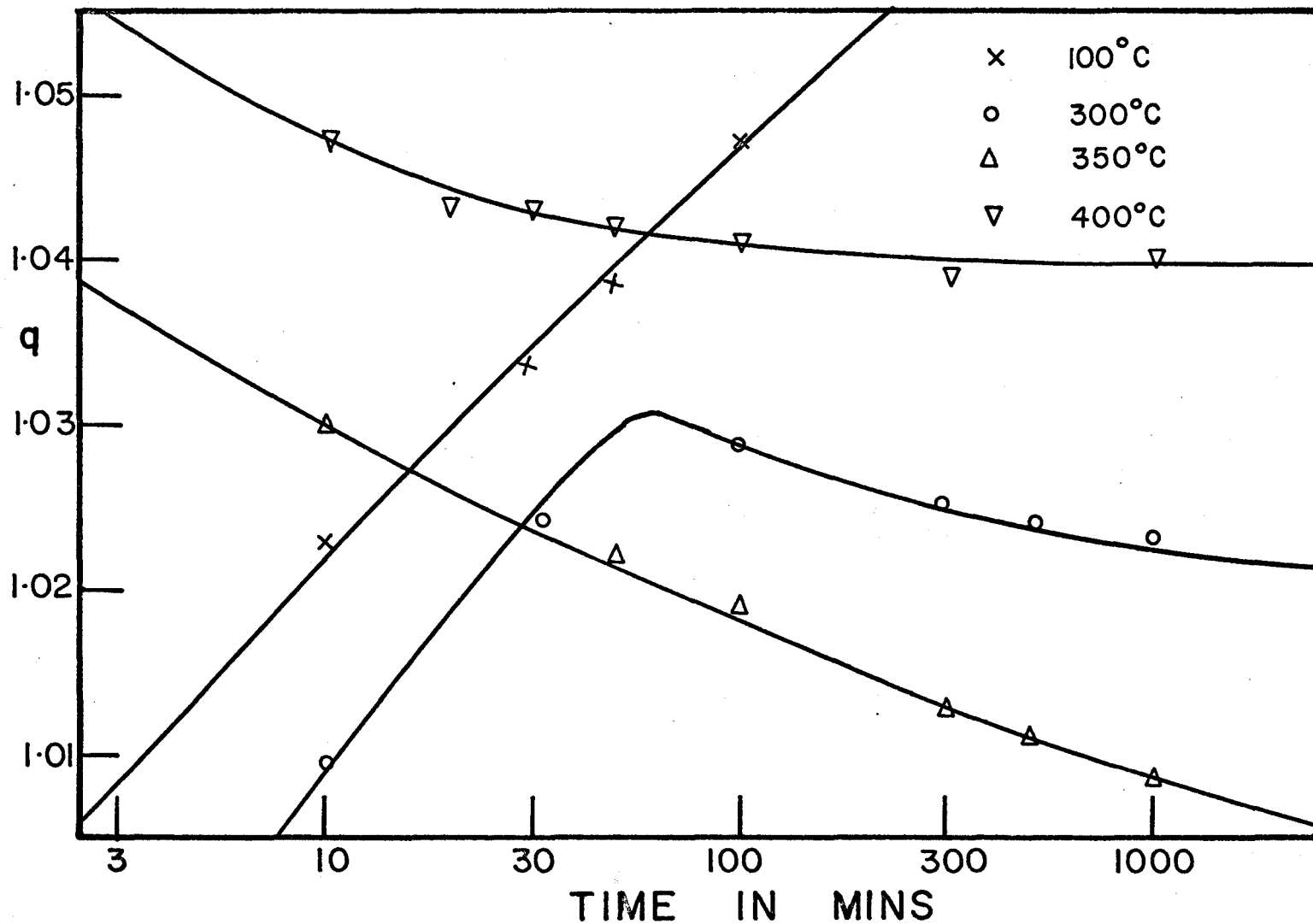


Fig. 8 Gas desorption and absorption in a NiP sample treated in water-vapour. The data shown is the result of Maxwell Garnett interpretations.

similar results were obtained with the only difference that the initial desorption period was longer (about 200 mins).

For nichrome films heated in air and water vapour at 100°C and 200°C, the results were found to be similar. However, the rates of desorption and absorption seem to be lower than in the case of nickel. Our attempts to deposit films of nickel and nichrome without any trapped nitrogen were not highly successful. The glass substrates were degassed up to one hour at high vacuum 4×10^{-8} torr before deposition. This resulted in substantially reducing the desorption period but it could not be eliminated completely.

When Ni-P films were heated in air at 100°C, 'q' showed an increase for about 200 mins. This may represent desorption of hydrogen which is present in the film as a by-product of the chemical deposition. The decrease in 'q' later on could be due to absorption of oxygen in the film. At 200°C, the process seems to be too rapid and our observations indicated only absorption on the surface. Our results on nickel phosphorous are generally in agreement with those of Marton and co-workers (5,6) who have observed that Ni-P does not grow a surface oxide film when treated in air below 280°C.

When Ni-P films were treated in water vapour at temperatures ranging from 100°C to 300°C, no oxide film was found to be present on the surface. The observed data at 100° and 200°C did not indicate any absorption even for long periods of

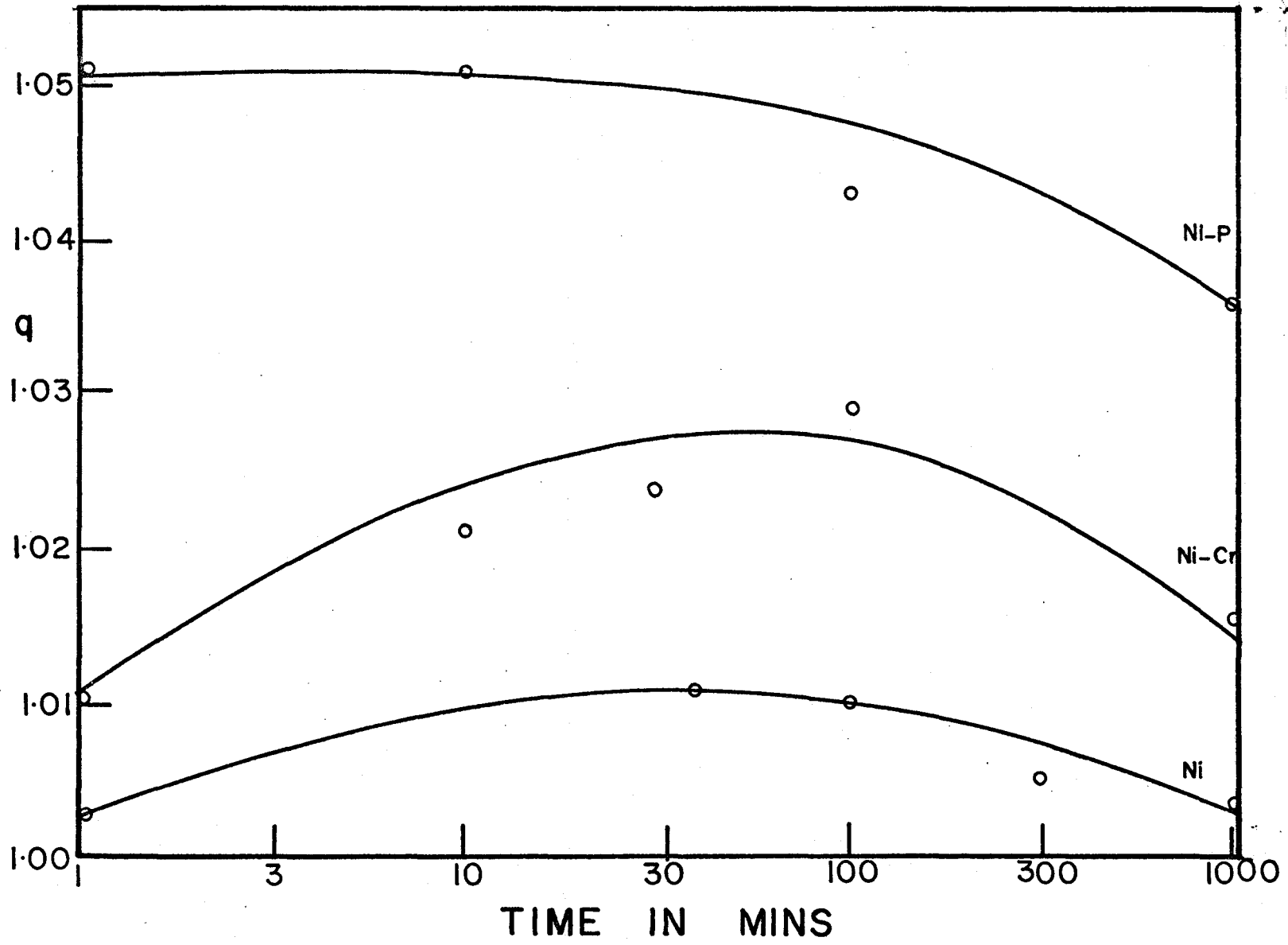


Fig. 9 Absorption and desorption of gases in Ni, Ni-P and Ni-Cr samples heated in air at 200°C.

treating. At 300°C, however, the initial desorption was followed by absorption after about 60 mins. Fig. (9) shows the results of Maxwell-Garnett analysis for films of Ni, Ni-Cr and Ni-P heated in air at 200°C.

4.4 Surface Film Interpretation

It was possible to interpret the ellipsometer observations Δ and ψ in terms of a surface oxide film for samples of nickel, nichrome and Ni-P treated at temperatures between 300°C and 400°C. However, this method of interpretation was not successful in the case of nickel films treated at 400°C for periods longer than 100 mins. No such problem was encountered with nichrome films in the temperature range up to 400°C.

We determined the optical constants of oxide free metals after each period of heating by second surface reflection. Thus knowing the optical constants of the metals, we could interpret the observed Δ and ψ at the free surface in terms of a surface film. It has already been shown that when nickel, nickel-phosphorous and nichrome are heated, they grow a surface oxide film. Fig. (10) shows the results of this interpretation for Ni-P samples. The thickness of oxide film has been plotted against the time of oxidation at various temperatures. From the same analysis, we also determined the optical constants of the oxide film. We found that the optical constants of the oxide film depend upon film thickness. Fig. (11) shows the variation of optical constants of the oxide with film thickness in the case of Ni-P sample. When Ni-P samples were

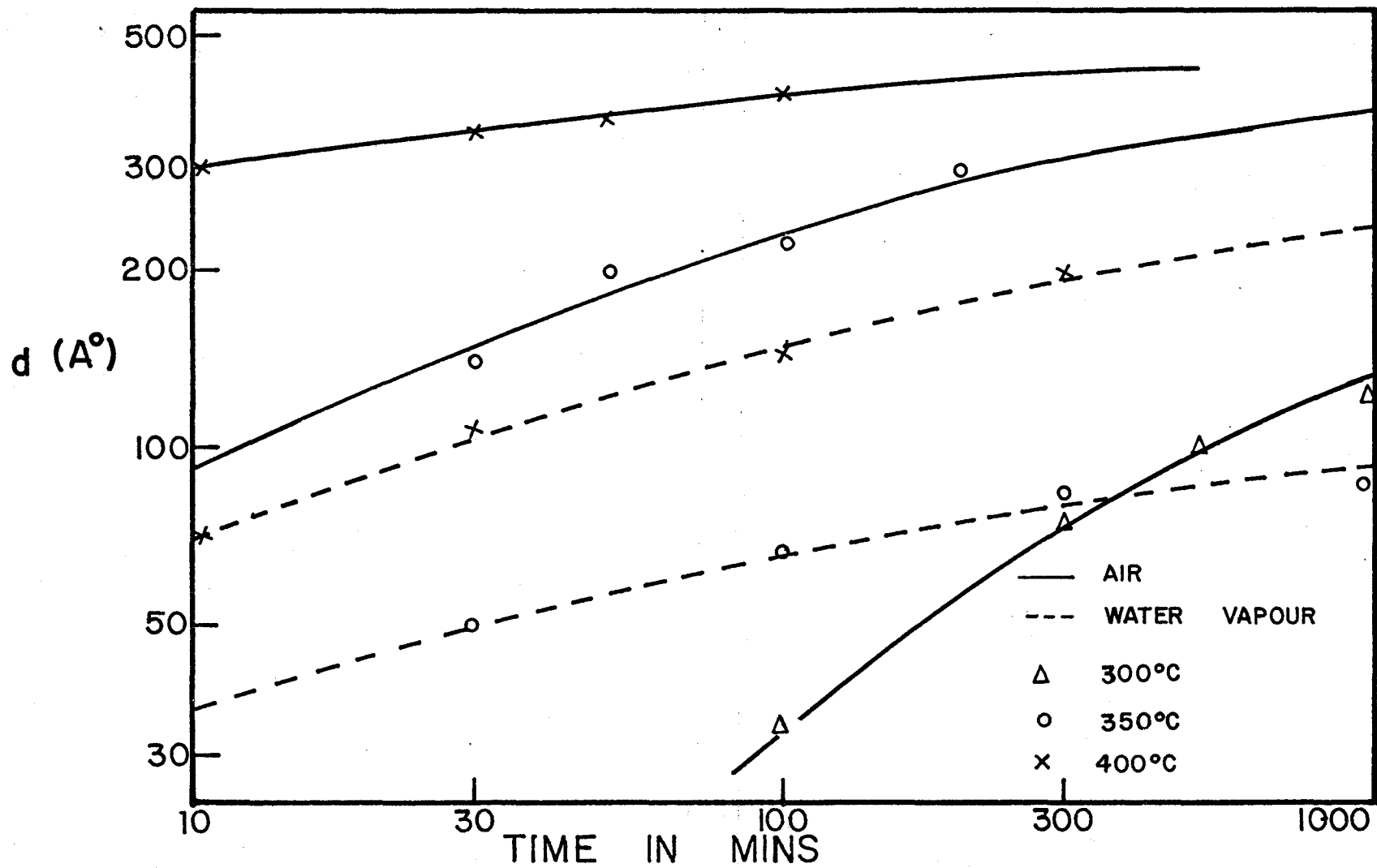


Fig. 10 Oxide film thickness on NiP sample as function of oxidation time at different temperatures in air and water vapour.

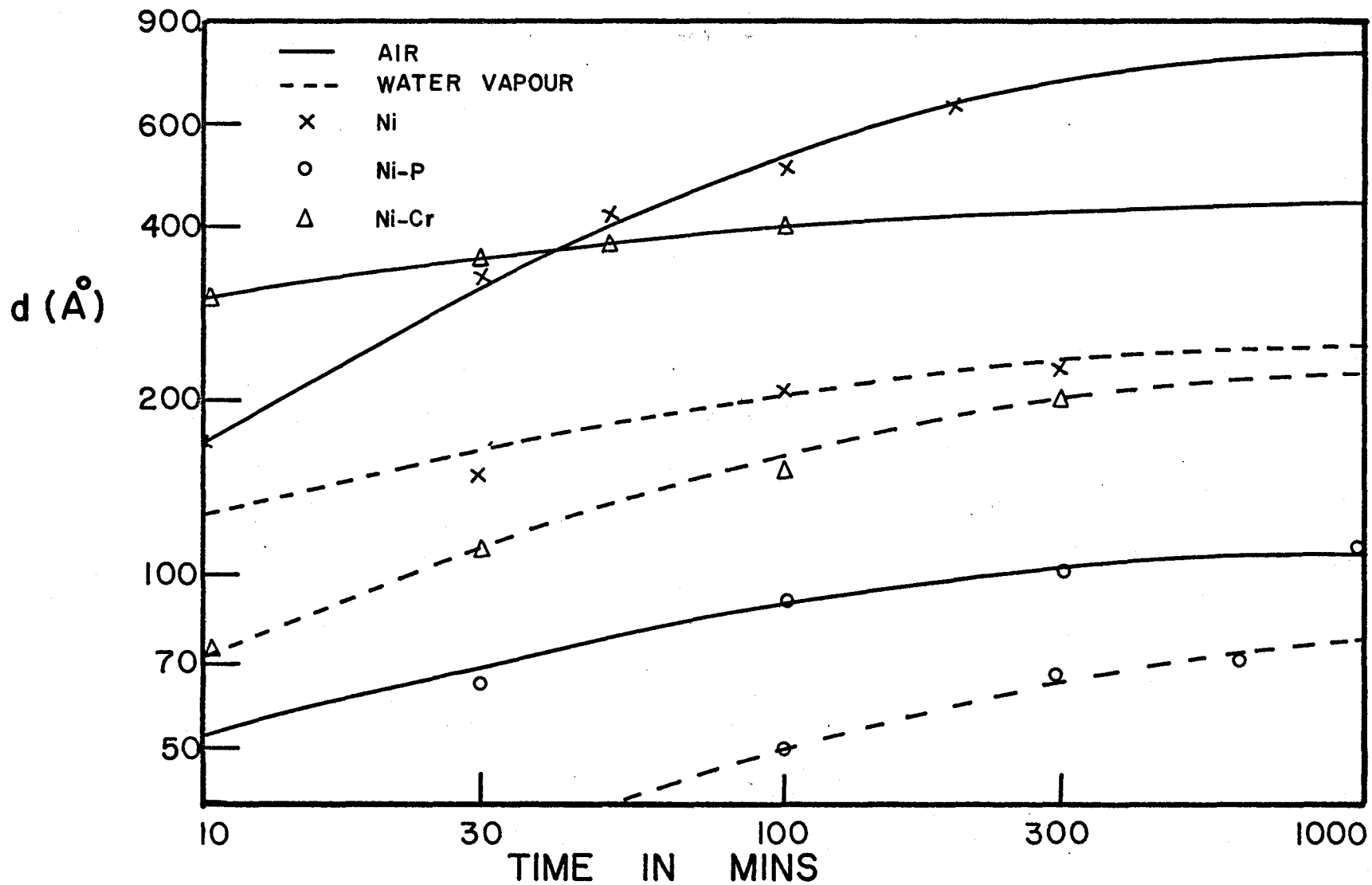


Fig. 11 Oxide film thickness on Ni, Ni-P and Ni-Cr as function of oxidation time in air and water vapour at 400°C.

treated in water vapour, results were similar to that in air except that the rate of growth of oxide films is less than it was in air.

For nickel and nichrome films treated in air and water vapour at temperatures from 300°C to 400°C, the results are quite similar to Ni-P. The growth of oxide is monotonic at temperatures above 300°C and is slower in water vapour than it is in air. The optical constants of the oxide film are thickness dependent. Fig. (12) illustrates the growth of oxide film on nickel, nichrome and Ni-P in air and water vapour at 400°C. Figs. (13a and 13b) show the variation of optical constants of oxide films with film thickness for Ni, Ni-Cr and Ni-P. From a study of figs. (12) and (13), the following inferences can be drawn.

- (a) Rate of oxidation is highest in nickel and lowest in nichrome.
- (b) The saturation values of optical constants of the oxide formed in all the three cases are very close. It is observed that n is the same, being 1.3 in all three cases, and the values of k are also not too far apart.

Powell and Spicer⁽⁴⁴⁾ found the optical constants of bulk nickel-oxide (NiO) to be $n = 2.36$, $k = 0.05$. Recently, Blondeau and co-workers^(45,46) determined the optical constants of NiO thin films. They used ellipsometric techniques for an in-situ study of anodic oxidation of nickel. For thin

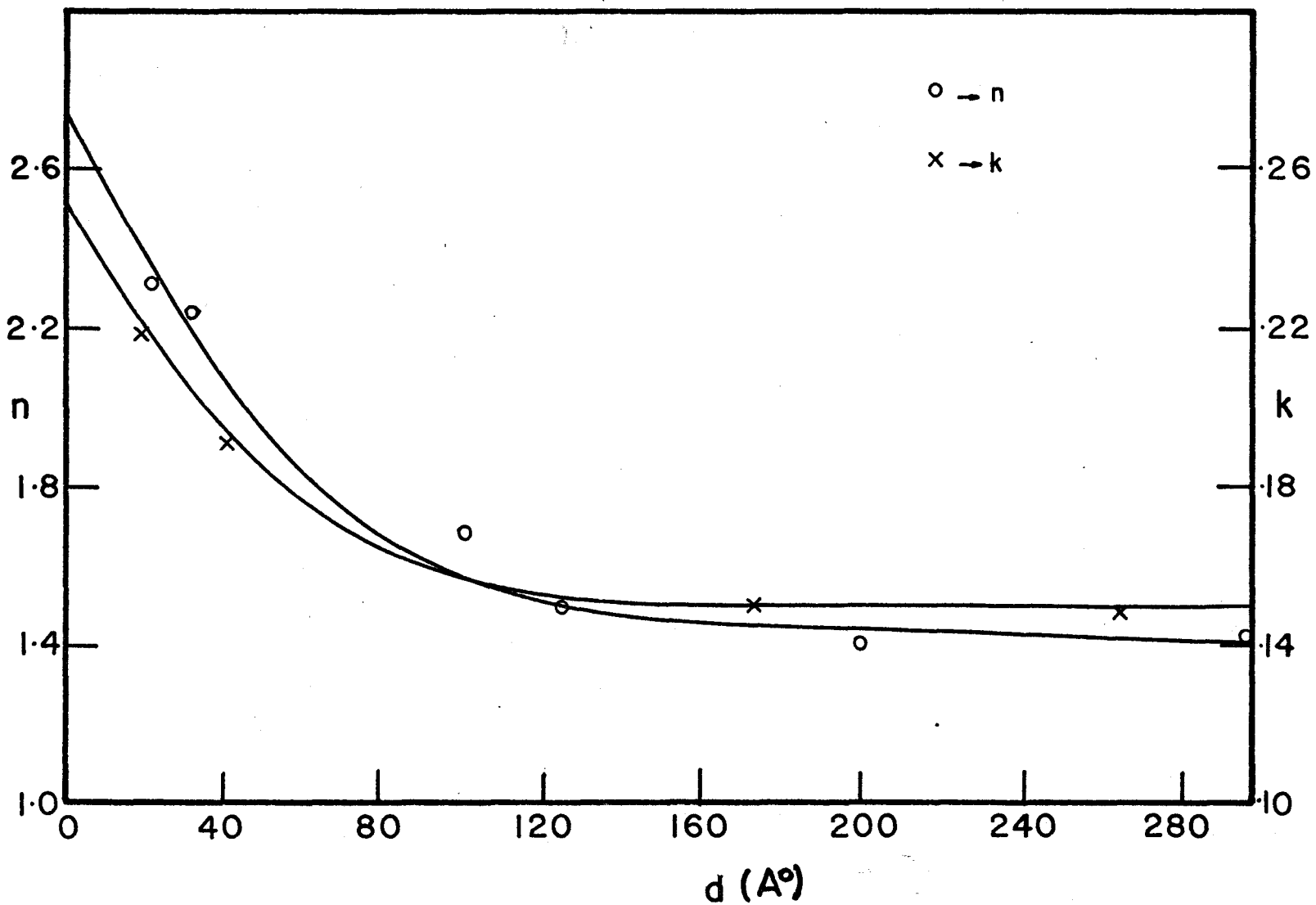


Fig. 12 Film thickness dependence of optical constants of oxide film on Ni-P sample.

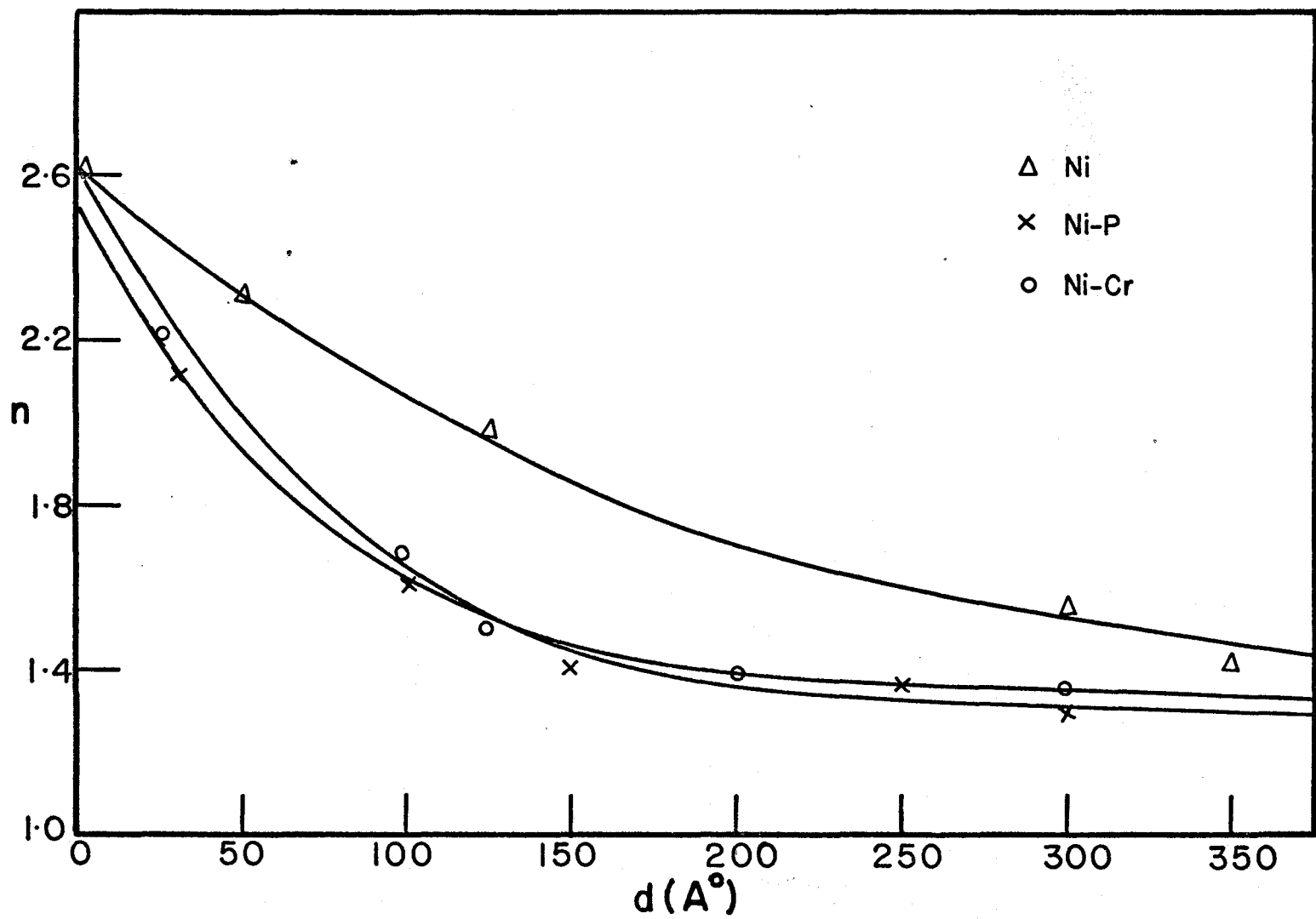


Fig. 13(a) Variation of refractive index of oxide films on Ni, Ni-P and Ni-Cr with film thickness. At large thicknesses the value approaches those of NiO.

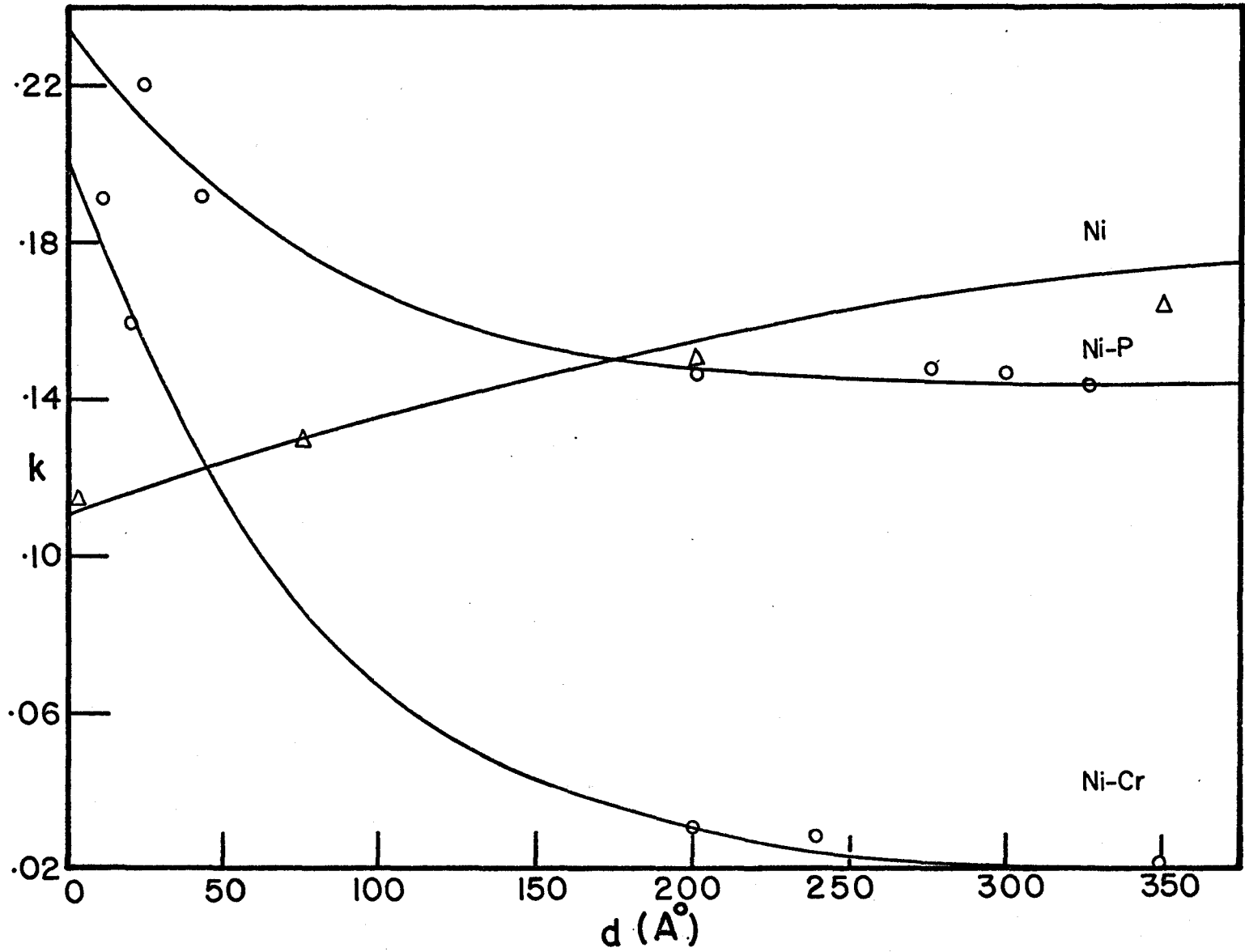


Fig. 13(b) Variation of extinction coefficient of oxide films on Ni, Ni-P and Ni-Cr with film thickness.

films of NiO they found the optical constants to be $n = 1.34$, $k = 0.04$. For thick films ($\approx 2400 \text{ \AA}$) the optical constants ($n = 2.32$, $k = 0.06$) approach the bulk values as reported by Powell and Spicer.

From a comparison of the optical constants of oxide films on Ni, Ni-Cr and Ni-P with those of NiO, it is apparent that NiO is the predominant phase in the oxide films.

4.5 Non-interpretable Data

We found that the observed Δ and ψ readings for Ni-P and nickel samples, treated in air at 400°C for periods longer than 100 mins and 300 mins respectively, could not be interpreted in terms of a surface oxide layer. These observations could not be analysed with the help of the Maxwell Garnett theory also. This behaviour can be explained if we assumed that oxygen penetrates greater thickness of the metal than is seen by the ellipsometer as the oxide layer. This assumption is supported by recent electrochemical studies on the corrosion properties of nickel annealed in air. It has been shown⁽⁴⁷⁾ that despite the removal of the oxide scale, the specimen exhibits enhanced reactivity and undergoes general corrosion. This behaviour has been interpreted as being due to dissolved oxygen beyond the main oxide scales. In ellipsometry, the surface film is required to be uniform and homogeneous in the plane of the film as well as in the thickness

direction. The observed variation of optical constants, n and k , with thickness of oxide film is an indication that the oxide film may not be homogenous in the thickness direction. Though we determined the optical constants of the metal after each period of treating by second surface reflection, yet failure to interpret the observed data in terms of an oxide film indicates that the optical constants of the unoxidised metal below the oxide layer are not the same as were calculated from observation at the second surface. This failure could also be due to inhomogeneties in the plane of the film. It is possible that these inhomogeneties could be caused by scaling, cracking and aggregating of the oxide film.

4.6 Oxidation in Different Oxygen Pressures

To gain a better understanding of the mechanism of oxidation in water vapour, we carried out oxidation of nickel, nichrome and nickel phosphorous at two different oxygen pressures besides that in air and water vapour. Oxygen and nitrogen were mixed at 1 lb. and 20 lb. pressures respectively to achieve 0.05 atm. pressure of oxygen. The two gases were then mixed in equal quantities at 10 lb. pressure. Samples of Ni, Ni-P and Ni-Cr were treated at 300°C and 400°C in these two gas mixtures separately. The thickness of the oxide film was calculated for each period of heating. The results of this study for nickel are presented in Fig. (14) where the thickness of the oxide film has been plotted versus oxygen partial pressures.

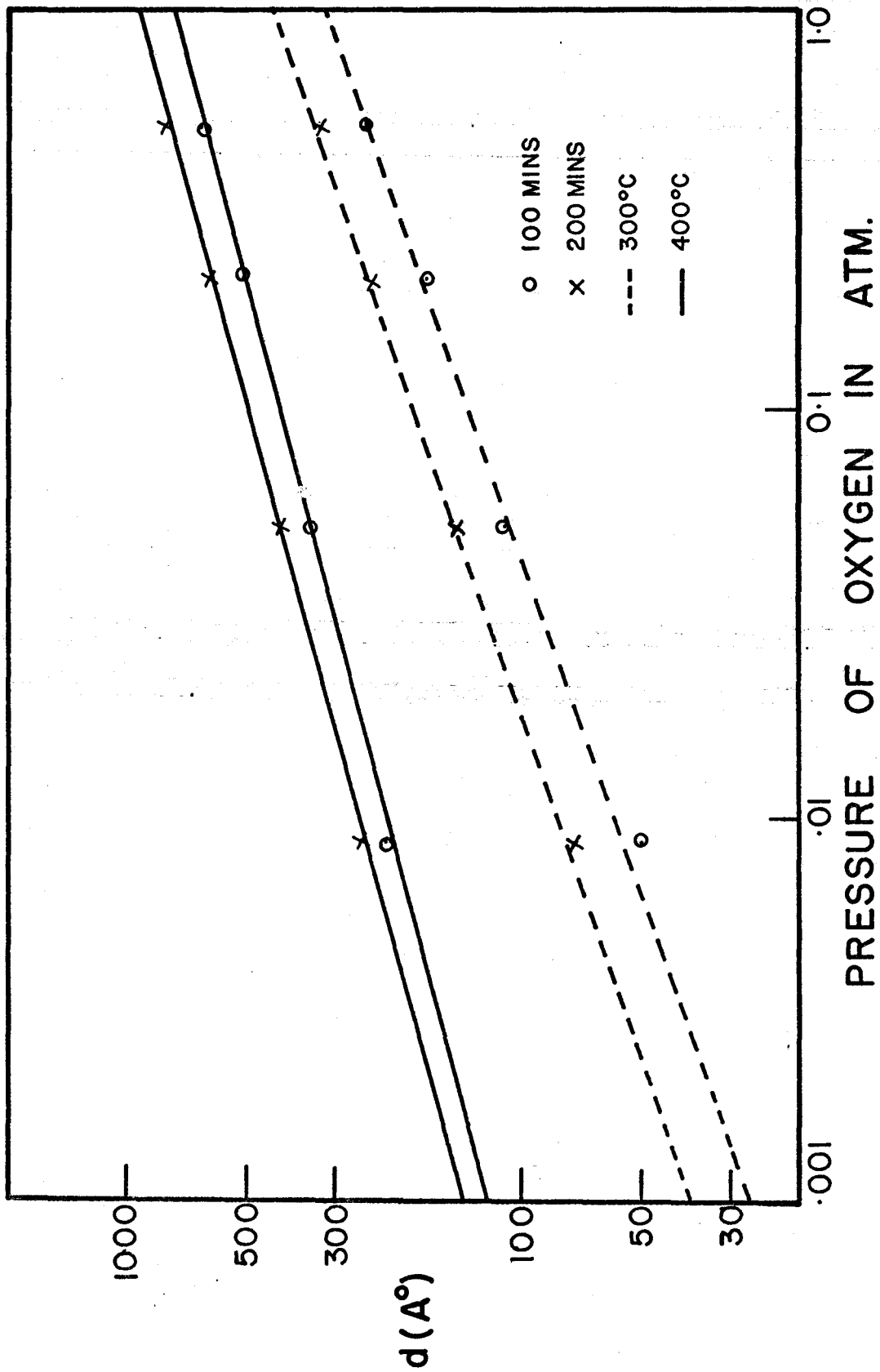


Fig. 14 Thickness of oxide film on Ni heated at 300°C and 400°C as a function of oxygen partial pressure.

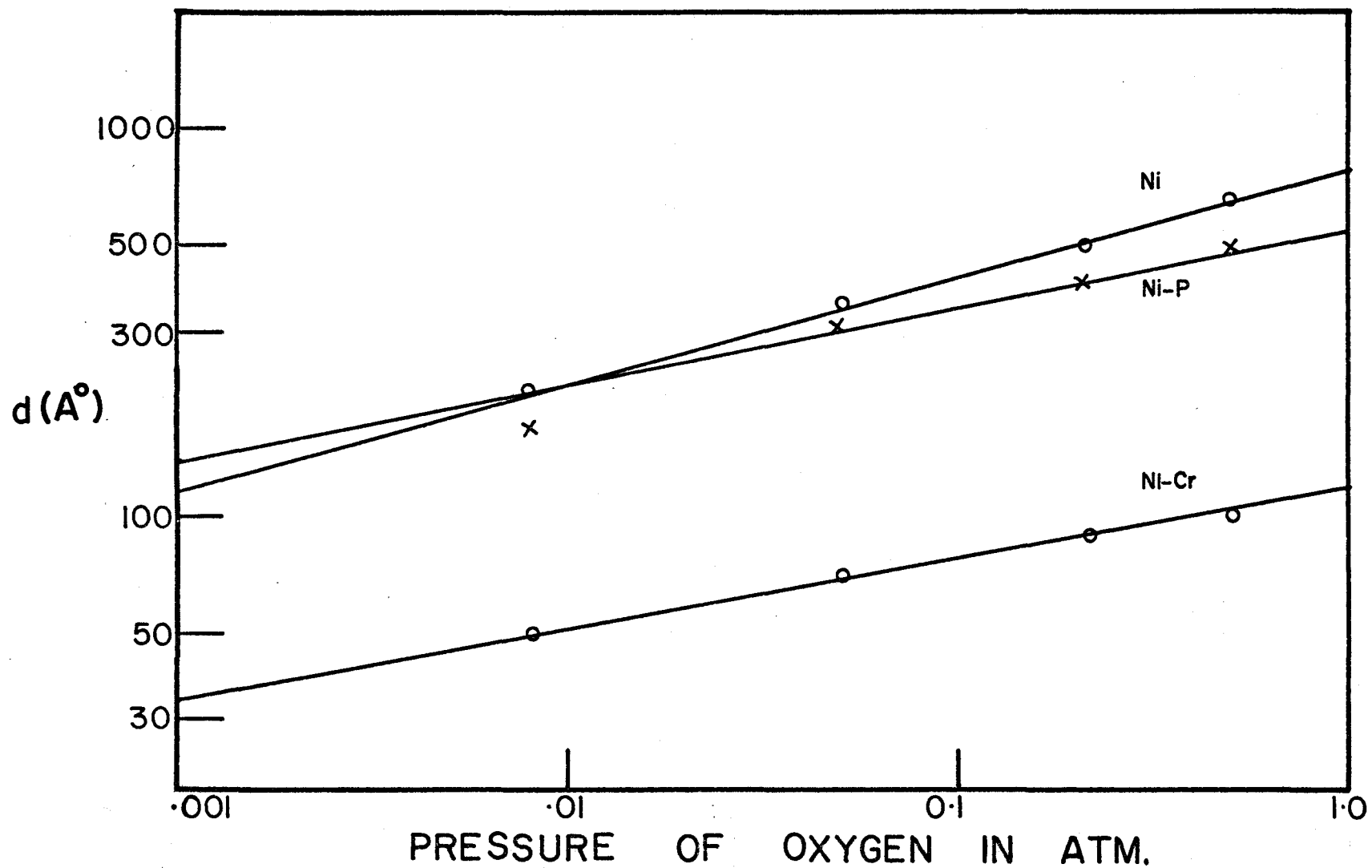


Fig. 15 Thickness of oxide film on Ni, Ni-P and Ni-Cr heated at 400°C for 100 mins. as a function of oxygen partial pressure.

The results indicate that the observed rate of oxidation in water vapour is nearly the same as is to be expected on the basis of partial pressure study. The oxidation in water vapour can be accounted for, within limits of experimental error, by the oxygen dissolved in water.

4.7 Effect of Water Vapours on Oxides

Three samples each of nickel, nichrome and Ni-P were first treated in air at 400°C for sufficient period of time to grow a thick ($\approx 500 \text{ \AA}$) oxide film. They were then subjected to treating in water vapour at 100°C and 200°C for periods of time up to 1000 mins. to study the effect of water vapour on the oxide layer. For all three samples of Ni-P, we found the thickness of the oxide film to decrease by 13 to 15%. The decrease in the oxide thickness is of the same order as the phosphorous content of Ni-P film. This suggests that the decrease is caused by removal of phosphorous from the surface by dissolution of P_2O_5 in water vapour. From a resistivity study of Ni-P films, Pai and Marton⁽⁶⁾ have found both NiO and P_2O_5 to be present in the oxide layer on the Ni-P films.

When samples of nickel with oxide layers on them were treated in water vapour at 100°C for 1000 mins, no change was noticed in the thickness of the oxide film. On treating in water vapour at 200°C for 1000 mins, two samples registered an increase of 5% in the thickness of the oxide film. The third sample did not show any change. This behaviour indicates

that nickel oxide is not affected by water vapour. The increase in oxide thickness could be due to further oxidation.

For nichrome films with oxide layers treated in water - vapour at 100° and 200°C for periods up to 1000 mins, no change in thickness of the oxide film was observed. This could mean that the oxide is not affected by water vapour and that oxidation of nichrome does not take place up to 200°C in water vapour.

CHAPTER V
CONCLUSIONS

- a. The optical constants of a freshly deposited film undergo change on heating. In most cases, n decreases and k increases, both saturating at longer times. In the case of NiP, this variation may be caused by compositional and crystalline changes which take place on heating. In nickel and nichrome, the variation may be ascribed to a change in the crystallite size and annealing of defects caused by heating. The effect is similar to the one caused by annealing the films in vacuum.
- b. The optical constants of the oxide layer on NiP, nickel and nichrome are nearly the same and similar to those of NiO. It is, therefore, concluded that nickel oxide (NiO) is the predominant phase in all the three cases.
- c. The decrease in the thickness of the oxide layer on NiP when heated in water vapour confirms the presence of P_2O_5 in the oxide.
- d. Oxidation in NiP, nickel and nichrome is a two stage process. At temperatures below 300°C , mainly oxygen is absorbed, while above this temperature a surface oxide layer forms.

e) The oxidation study at various oxygen pressures is not conclusive. The experimental error in the determination of thickness is of the same order of magnitude as the deviation of some of the data points from the curve. The data indicates, however, that water vapour does not play a vital role in the oxidation process. The oxidation in water vapour may be attributed to the presence of dissolved oxygen in water.

f) Oxygen seems to penetrate to a greater depth in the metal than that calculated to be the thickness of the oxide layer. The boundary between the oxide layer and unoxidised metal seems to be rather diffused. This may be due to the presence of an oxygen rich metal region between the two layers.

APPENDIX I

DETERMINATION OF SUBSTRATE OPTICAL CONSTANTS
BY SECOND SURFACE REFLECTION

In this method, the metal is deposited as a film on one side of a plane, parallel sided glass substrate. Consider a parallel beam of plane polarised light, with plane of polarisation at 45° to the plane of incidence. The reflection and transmission coefficients for the p and s components at the air glass and glass metal interfaces, denoted by r_1 , t_1 and r_2 , t_2 respectively are given by equations (8-11). The transmission coefficients in the opposite direction (glass \rightarrow air) are represented by t_p' and t_s' . The amplitudes of the reflected and transmitted beams are as shown in figure . For the first reflected beam from the metal surface, the amplitudes of the p and s components are given by -

$$R_p = t_p \cdot t_p' \cdot r_2$$

$$R_s = t_s \cdot t_s' \cdot r_2$$

Let ϕ_0 , Δ_0 and ψ_0 be the observed parameters when this beam alone is considered. It is required to find $\bar{\phi}$, $\bar{\Delta}$ and $\bar{\psi}$ for the reflection of this beam at the metal surface at the point B. It is easily seen that $\bar{\phi}$ and $\bar{\Delta}$ are given by

$$\bar{\phi} = \phi_1 = \sin^{-1} \left[\frac{\sin \phi_0}{n_1} \right]$$

$$\bar{\Delta} = \Delta_0$$

The ratio of the amplitudes of the p and s components in this beam is given by

$$\frac{R_p}{R_s} = \frac{t_p \cdot t_{p'} \cdot r_{2p}}{t_s \cdot t_{s'} \cdot r_{2s}} = \tan \psi_0.$$

From this change in amplitude on reflection at the metal surface at B can be obtained as

$$\frac{r_{2p}}{r_{2s}} = (\tan \psi_0) \frac{t_s \cdot t_{s'}}{t_p \cdot t_{p'}} = \tan \bar{\psi}$$

Hence

$$\bar{\psi} = \tan^{-1} \left[\tan \psi_0 \frac{t_s \cdot t_{s'}}{t_p \cdot t_{p'}} \right].$$

Having thus determined $\bar{\phi}$, $\bar{\Delta}$ and $\bar{\psi}$, the optical constants of the metal can be calculated using equations (17-19)..

APPENDIX II

POLARISATION FIELD OF SPHERICAL METAL CRYSTALLITES

It has been assumed that the system consists of spherical metal particles embedded in a dielectric medium. The size of the metal particles is small compared to the film dimensions and wavelength of light used.

When this system is subjected to an electromagnetic field \bar{E} the metallic crystallites will be polarised giving rise to a polarisation field \bar{E}_s . The field contributed by the dipoles may be divided into two parts:

- (a) that arising from a spherical region, around the point in question of radius large enough to contain many dipoles.
- (b) that from the remainder of the medium.

If the diameter of the sphere is small as compared to the wavelength of light used, then the contribution from (a) is zero. The field due to material outside the sphere is $\frac{4\pi}{3} \bar{P}$ where \bar{P} is the electric moment per unit volume of the medium. The total field \bar{F} is therefore given by

$$\bar{F} = \bar{E} + \bar{E}_s = \bar{E} + \frac{4\pi}{3} \bar{P}. \quad (1)$$

Since the distribution of spheres is assumed to be random, the medium may be treated as isotropic and we may write $P = k \cdot N \bar{E}$, when k is a constant and N is the number of crystallites per unit volume.

Writing $F = \epsilon \bar{E}$, we obtain

$$\frac{\epsilon-1}{\epsilon+2} = \frac{4\pi}{3} k \cdot N .$$

Since we know that $\epsilon = n^2$, equation can be written as

$$\frac{n^2-1}{n^2+2} \cdot \frac{1}{\rho} = \text{constant}$$

where ρ is the density of the crystallites in the medium.

The thin film may be represented by a volume fraction 'q' of spheres of index \tilde{N} in a medium of refractive index nearly equal to unity. The effective index \tilde{N}_e of the system is given by

$$\frac{\tilde{N}_e^2-1}{\tilde{N}_e^2+2} = 'q' \cdot \frac{\tilde{N}^2-1}{\tilde{N}^2+2} .$$

REFERENCES

- (1) 'Optical Properties of Thin Solid Films' - O.S. Heavens Butterworths, London. p. 123-130 (1955).
- (2) D. K. Burge and H. E. Bennet, J. Opt. Soc. Am. 54, 564A (1964).
- (3) J. P. Marton and M. Schlesinger, J. Electrochem. Soc. 115, 16 (1968).
- (4) S. T. Pai, J. P. Marton and J. D. Brown. J. Appl. Phys. 43, 282 (1972).
- (5) J. P. Marton and E. C. Chan, J. Appl. Phys. 43, 1681 (1972).
- (6) S. T. Pai and J. P. Marton, J. Apply. Phys. to be published.
- (7) E. A. Gulbranson and K. F. Andrew, J. Electrochem Soc. 101, 128 (1954).
- (8) Ibid. 104, 451 (1957).
- (9) G. C. Wood, I. G. Wright and J. M. Ferguson, Corr. Sci. 5, 645 (1965).
- (10) K. Hauffe, L. Pethe, R. Schmidt and S. Roy Morrison, J. Electrochem. Soc. 115, 456 (1968).
- (11) N. Birks and H. Rickert, J. Inst. Metals 91, 308 (1963).
- (12) D. L. Douglass, Corr. Sci. 8, 665 (1968).
- (13) 'Oxidation of Metals and Alloys' - O. Kubaschewski and B. E. Hopkins, Butterworths, London. (1967) p. 135-36.
- (14) G. Bandel, ARch. Eisenhuttenw, 15, 271 (1941).
- (15) W. Baukloh and P. Funke, Korros. Metallsch., 18, 126 (1942).
- (16) Reference 13 above, p. 271.
- (17) A. Rahmel, Corr. Sci. 5, (12), 815 (1965).
- (18) S. Roberts, Phys. Rev. 114, 104 (1959).
- (19) M. R. Meyerson, 'Nickel and its alloys', N.B.S. Circular 485 (1950).

- (20) 'Optical Properties of Solids' - Frank Stern, Solid State Physics, Vol. 15, 1963 (Academic Press).
- (21) Reference 1 above, p. 51-53.
- (22) Ibid. p. 55-57.
- (23) 'Ellipsometry in the Measurement of Surfaces and Thin Films' N.B.S. Misc. Publications no. 256, 1964.
- (24) M. Born and E. Wolf- Principles of Optics. Pergamon Press, London p. 40 (1959).
- (25) A. Rothen, Rev. Sci. Instr. 16, 26 (1945).
- (26) R. J. Archer, J. Opt. Soc. Am. 52, 970 (1962).
- (27) A. B. Winterbottom - Optical Studies of Metal Surfaces. Trondheim p. 50-56 (1955).
- (28) Symposium on recent developments in ellipsometry. Surface Science Vol. 16 (1969).
- (29) F. L. McCrackin, E. Passaglia, R. Stromberg and H. L. Steinberg, J. Res. Natl. Bur. Std. 67A, 363 (1963).
- (30) F. L. McCrackin and J. Colson, N.B.S. Tech. note 242 (1964).
- (31) A. N. Saxena, Appl. Phys. Lett. 7, 113 (1965).
- (32) K. H. Zaininger and A. G. Revesz, J. Phys. 25, 208 (1964).
- (33) K. Vedam, W. Knausenberger and F. Lukes, J. Opt. Soc. Am. 59, 64 (1969).
- (34) M. Ruiz-Urbieta, E. M. Sparrow and E.R.G. Eckert, J. Opt. Soc. Am. 61, 351 (1971).
- (35) J. Shewchun and E. C. Rowe, J. Appl. Phys. 41, 4128 (1970).
- (36) Samuel S. So and K. Vedam, J. Opt. Soc. Am. 62, 16 (1972).
- (37) J. C. Maxwell Garnett, Phi. Trans. 203, 305 (1904).
Ibid. 205A, 237 (1906).

- (38) J. P. Marton, Ph.D. Thesis (1968), University of Western Ontario, London.
- (39) R. S. Sennett and G. D. Scott, J. Opt. Soc. Amer. 40, 203 (1950).
- (40) J. Shewchun, McMaster University, Hamilton. Unpublished results.
- (41) A. Nag and L. Ward, J. Phys. 4, 829 (1971).
- (42) J. R. Adams and K. K. Rao, Surface Sci. 16, 382 (1969).
- (43) R.J. Lederich and J. J. Bellina, J. Opt. Soc. Am. 60, 1697 (1970).
- (44) R.J. Powell and W.E. Spicer, Phys. Rev. 2, 2182 (1970).
- (45) G. Blondeau, M. Froment, A. Hugot-LeGoff, C.R. Acad. Sc. 271, 795 (1970).
- (46) G. Blondeau, M. Froment, M. Froelichov, A. Hugot-LeGoff, C.R. Acad. Sci. 274, 365 (1972).
- (47) M. Zamin, M. Eng. thesis, p. 110., McMaster University, Hamilton.
- (48) E. C. Chan and J. P. Marton, J. Appl. Phys. 43, 4027 (1972).
- (49) A. Vasicek, J. Opt. Soc. Am. 37, 145, (1947).